Stochastic Environmental Research and Risk Assessment (2018) 32:1993–2023
https://doi.org/10.1007/s00477-018-1523-3

ORIGINAL PAPER

Synthetic design hydrographs for ungauged catchments: a comparison of regionalization methods

Manuela I. Brunner[1,2] · Reinhard Furrer[3,4] · Anna E. Sikorska[1,5] · Daniel Viviroli[1,6] · Jan Seibert[1,7] · Anne-Catherine Favre[2]

Published online: 24 February 2018
© Springer-Verlag GmbH Germany, part of Springer Nature 2018

Abstract
Design flood estimates for a given return period are required in both gauged and ungauged catchments for hydraulic design and risk assessments. Contrary to classical design estimates, synthetic design hydrographs provide not only information on the peak magnitude of events but also on the corresponding hydrograph volumes together with the hydrograph shapes. In this study, we tested different regionalization approaches to transfer parameters of synthetic design hydrographs from gauged to ungauged catchments. These approaches include classical regionalization methods such as linear regression techniques, spatial methods, and methods based on the formation of homogeneous regions. In addition to these classical approaches, we tested nonlinear regression models not commonly used in hydrological regionalization studies, such as random forest, bagging, and boosting. We found that parameters related to the magnitude of the design event can be regionalized well using both linear and nonlinear regression techniques using catchment area, length of the main channel, maximum precipitation intensity, and relief energy as explanatory variables. The hydrograph shape, however, was found to be more difficult to regionalize due to its high variability within a catchment. Such variability might be better represented by looking at flood-type specific synthetic design hydrographs.

Keywords Regionalization · Ungauged catchments · Design hydrographs · Flood estimation · Regression trees

1 Introduction

Flood estimates for a given return period are required for many engineering problems, such as the construction of retention basins and weirs or drawing hazard maps (Grimaldi and Petroselli 2015; Mediero et al. 2010; Yue and Rasmussen 2002). Two types of approaches exist for the construction of design floods for a predefined return period in catchments, where runoff information is available (Smithers 2012): rainfall-runoff modeling and flood frequency analysis. Rainfall-runoff models describe how rainfall is transferred into runoff. On the one hand, excess rainfall that becomes direct runoff is modeled by considering losses through infiltration, interception, and surface storage (e.g. via runoff coefficients or infiltration equations). On the other hand, a transfer function describes how this excess rainfall is transferred into runoff (e.g. unit hydrograph (Singh et al. 2014)). These methods are based on the assumption that the return period of the rainfall input corresponds to the return period of the resulting design

✉ Manuela I. Brunner
manuela.brunner@geo.uzh.ch

[1] Department of Geography, University of Zurich, Zurich, Switzerland

[2] Université Grenoble-Alpes, CNRS, IRD, IGE, Grenoble INP, Grenoble, France

[3] Department of Mathematics, University of Zurich, Zurich, Switzerland

[4] Department of Computational Science, University of Zurich, Zurich, Switzerland

[5] Department of Hydraulic Engineering, Warsaw University of Life Sciences, SGGW, Warsaw, Poland

[6] belop gmbh, Sarnen, Switzerland

[7] Department of Earth Sciences, Uppsala University, Uppsala, Sweden

hydrograph (Chapman and Maxwell 1996), which is not always the case (Viglione et al. 2009).

Contrary to rainfall-runoff modeling, flood frequency analysis is based solely on observed runoff data (Meylan et al. 2012) and thus overcomes this assumption. However, the focus of flood frequency analysis usually lies on the hydrograph peaks (Ahn and Palmer 2016). Such a univariate analysis is not sufficient for design tasks where the storage of the flood water is of concern. In this case, information on the whole flood hydrograph is required (Pilgrim 1986). A first step towards the construction of flood hydrographs is a bivariate flood frequency analysis, which is jointly looking at peak discharges and hydrograph volumes considering their dependence (Requena et al. 2013; Shiau et al. 2006). Bivariate flood quantiles can then be combined with a dimensionless unit hydrograph (Serinaldi and Grimaldi 2011) that describes the shape of the design event. Brunner et al. (2017b) proposed a statistical flood frequency model for the construction of synthetic design hydrographs (SDHs) which combines bivariate design quantiles with a unit hydrograph represented as a probability density function (Bhunya et al. 2011). Such SDHs provide information on the hydrograph peak, the hydrograph volume, and the entire hydrograph shape. The SDH construction model is useful in gauged catchments, where runoff information is available for design hydrograph estimation. Yet, it is not directly applicable in ungauged catchments where runoff is not measured or in catchments where the record is too short to estimate reliable statistics (Ahn and Palmer 2016; Blöschl et al. 2013). Therefore, a regionalization model is needed for describing how the SDH parameters can be transferred from gauged to ungauged catchments. A range of different data types has previously been regionalized from gauged to ungauged catchments: parameters of continuous rainfall-runoff models (see reviews by He et al. (2011) and Razavi and Coulibaly (2013)), unit hydrograph parameters (Tung et al. 1997), daily flows (Farmer 2016; Kokkonen et al. 2003; Sefton and Howarth 1998), low flows (Laaha et al. 2014; Longobardi and Villani 2008; Salinas et al. 2013), flow duration curves (Boscarello et al. 2016; Cheng et al. 2012; Sauquet and Catalogne 2011), flood quantiles (GREHYS 1996; Merz and Blöschl 2004; Ouarda et al. 2001; Skoien et al. 2006), and flood event durations (Cipriani et al. 2012). However, the identification of the most suitable regionalization method is likely context dependent (Ali et al. 2012). To our knowledge, no method has so far been proposed for the regionalization of a design flood hydrograph that is solely based on runoff observations and represents both the peak and volume of the hydrograph and its shape while providing information on the event's frequency via the return period. In this study, we therefore focus on finding an appropriate method for the regionalization of design flood hydrographs to ungauged catchments. This method can subsequently be applied by engineers to derive SDHs in catchments where runoff measurements are not available. Our specific research questions were:

1. Which is the most appropriate regionalization method for transferring SDHs from gauged to ungauged catchments?
2. Do nonlinear regression techniques, such as random forest, bagging, and boosting, perform better compared to classical regionalization techniques?
3. Which catchment characteristics are most important for the prediction of SDH parameters in ungauged catchments?

To address these questions, we tested and compared 24 suitable regionalization methods that have been proposed either in the hydrological or statistical literature. These included methods establishing a relationship between catchment characteristics and design hydrograph parameters, approaches based on spatial proximity, and methods related to the building of homogeneous regions. Besides commonly used regionalization methods such as multiple linear regression and various kriging approaches, we also tested three nonlinear regression methods, i.e., bagging, random forest, and boosting, which have so far only rarely been used in hydrological regionalization studies. Regression trees have been used by Laaha and Blöschl (2006) to regionalize low flows and bagging has been used by Shu and Burn (2004) to regionalize index floods and 10-year flood quantiles. Unlike other, commonly applied methods, nonlinear regression approaches allow the consideration of hydrological processes that are nonlinear and exhibit a high degree of spatial variability (Aziz et al. 2015).

The nonlinear regression methods tested here are tree-based. They split the space of explanatory variables into a number of regions containing observations with similar response values (Strobl et al. 2009). To make a prediction for a given observation, the mean or the mode of the observations in its region can be used. The set of splitting rules used to segment the space of explanatory variables can be summarized in a tree (Hastie et al. 2008). Tree-based methods have the advantage that the model outcome is unaffected by monotone transformations of the input data and different measurement scales among explanatory variables. Furthermore, irrelevant explanatory variables are seldomly selected. The hierarchical structure of a tree ensures that the response to one input variable depends on values of inputs higher in the tree, which allows for the automatic modeling of interactions between explanatory variables (Elith et al. 2008). A tree-based method might produce good predictions on the set used to fit the model, but is likely to overfit the data, leading to a poor test

performance and high variance (James et al. 2013). Combining a large number of trees into an ensemble (Strobl et al. 2009), using bagging, random forest, or boosting methods, leads to a smoothing of the estimated response surface, results in an improvement in prediction accuracy, and reduces variance compared to applying just one single tree (James et al. 2013). Variance can be reduced by bootstrap aggregation (bagging) which takes many random samples from the population using bootstrap techniques, builds a separate prediction model using each sample, and averages the resulting predictions (Liaw and Wiener 2002). If there is a strong explanatory variable in the set, most trees in the set of trees obtained by bagging will use this explanatory variable in the top split. Random forests overcome this problem by forcing each split to consider only a subset of the explanatory variables, which corresponds to a decorrelation of the trees (Breiman 2001; James et al. 2013). While bagged trees and random forest reduce variance compared to single trees, they cannot achieve any bias reduction because each tree is based on a bootstrap sample that has the same distribution as the original data set (Elith et al. 2008). This problem can be overcome by using boosted regression trees. Boosted regression trees combine the strengths of the two algorithms regression trees and boosting (Freund and Schapire 1996; Friedman 2001, 2002). Boosting is a forward, stagewise procedure in which models (here regression trees) are fitted iteratively to the data using appropriate methods focusing on observations modelled poorly by the existing collection of trees (Hofner et al. 2009). This stagewise procedure, where successive trees depend on previous trees, distinguishes boosting from bagging.

2 Data

2.1 Study catchments

This regionalization study was performed using runoff and catchment characteristics data from 163 Swiss catchments (Fig. 1, and the Table in the "Appendix") with a wide range of catchment characteristics and flood behaviors. The selected catchments have hourly flow series of at least 20 years in duration ranging up to 53 years. The application of the hydrograph construction procedure presented in the next paragraph is suitable for catchments with records of at least 20 years, especially, if longer return periods such as $T = 100$ years are of interest (Deutsche Vereinigung für Wasserwirtschaft Abwasser und Abfall 2012). The catchments' runoff is neither altered by regulated lakes upstream or inland canals nor by urbanized areas. The catchments are small to medium-size (6–1800 km^2), situated between 400 and 2600 m.a.s.l. (mean elevation), and either with no or only a few areas with glaciers.

2.2 SDH parameters

We constructed hydrographs for the study catchments using the method for a catchment specific construction of synthetic design hydrographs (SDHs) proposed by Brunner et al. (2017b). They form the data-and validation basis for the regionalization study and their parameters are provided in Table 5 in "Appendix". The method uses observed runoff data, models the hydrograph shape using a probability density function (PDF), and considers the dependence between the design variables, peak discharge (Q_p) and hydrograph volume (V) which are used for the estimation of the bivariate design quantiles Q_T and V_T. It consists of ten steps which are shortly summarized here:

1. Flood sampling using a peak-over-threshold approach as proposed by Lang et al. (1999). The threshold for the peak discharge was chosen iteratively to fulfill a target condition of four events per year on average which is a trade-off between maximizing the information content in the sample and keeping the assumption of independence between events. The independence between successive events was additionally ensured by prescribing a minimum time interval of 72 h between them;
2. Baseflow separation using the recursive digital filter proposed by Eckhardt (2005) whose two parameters need to be estimated for each catchment;
3. Normalization of the hydrograph so that both the base width and the volume of the modified hydrographs were equal to one;
4. Identification of the median hydrograph as a representative normalized hydrograph (RNH) using the h-mode depth for functional data (Cuevas et al. 2007);
5. Fitting of a lognormal probability density function (PDF) (Rai et al. 2009; Yue et al. 2002) to the RNH. The shape of a normalized hydrograph can be fitted by a probability density function (PDF) because both the area under the normalized hydrograph and the area under the PDF are equal to one and because probability density functions can take various shapes;
6. Dependence modeling between peak discharges and hydrograph volumes using the Joe copula (Genest and Favre 2007; Joe 1997). The Joe copula is described by:

$$C(u,v) = 1 - \left[(1-u)^{\theta} + (1-v)^{\theta} - (1-u)^{\theta}(1-v)^{\theta}\right]^{\frac{1}{\theta}}, \quad (1)$$

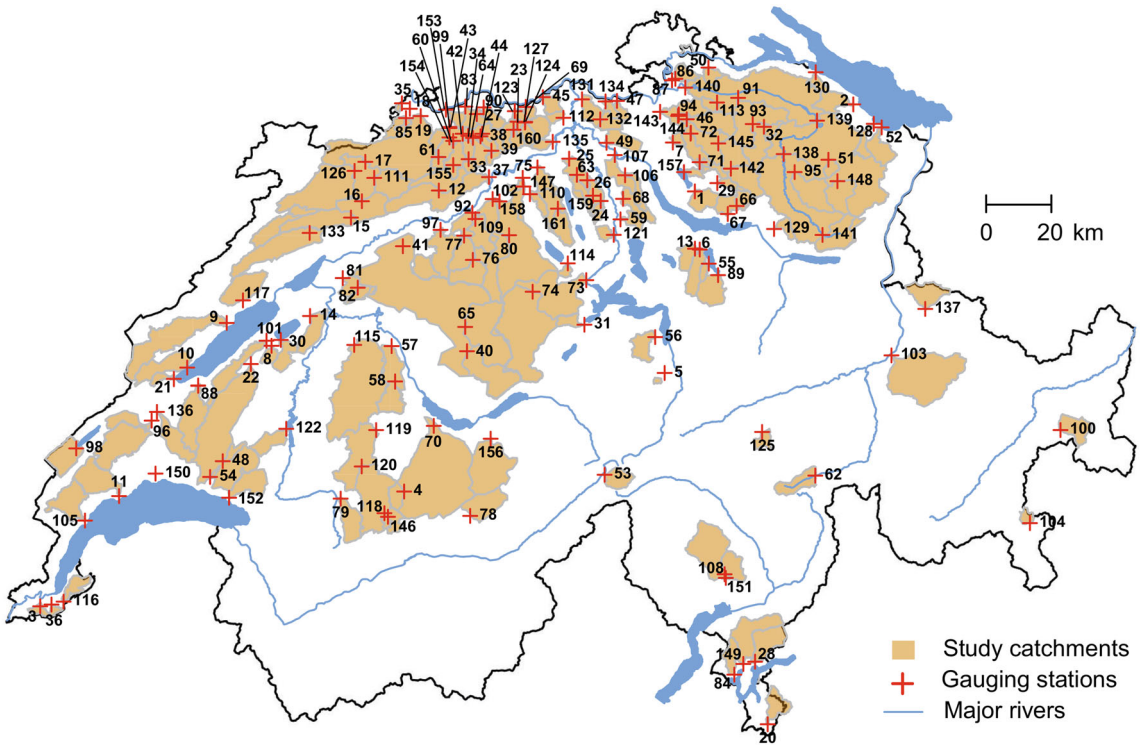

Fig. 1 Map of the 163 Swiss study catchments used for testing different regionalization methods. The gauging stations are indicated as red crosses and labeled with the catchment ID given in the table in "Appendix"

where θ is the copula parameter, $u = F_X(x)$ and $v = F_Y(y)$ are uniformly distributed between 0 and 1, and their dependence is modeled by the copula C.;

7. Choice of a return period definition according to the problem at hand (Brunner et al. 2016). Here, we used the joint OR return period assuming that both peak discharge and hydrograph volume are equally important for the problem at hand. The joint OR return period is defined as follows:

$$T(x,y) = \frac{\mu_0}{Pr[X > x \vee Y > y]} = \frac{\mu_0}{1 - F_X(x) - F_Y(y) + F_{XY}(x,y)} = \frac{\mu_0}{1 - C(u,v)}, \quad (2)$$

where X and Y are random variables, C is a copula, x and y are given thresholds, μ_0 is the inter-arrival time between two successive events $u = F_X(x)$ and $v = F_Y(y)$, and F_X, F_Y, and F_{XY} are the marginal and joint distribution functions of the random variables respectively;

8. Estimation of the design variable quantiles peak discharge (Q_T) and hydrograph volume (V_T) for the chosen return period using their marginal distributions. A marginal Generalized Pareto distribution (GPD) was used for peak discharges and a Generalized extreme value (GEV) distribution for the hydrograph volumes. The GPD model has three continuous parameters: a location parameter μ in $\mathbb{R}$, a scale parameter $\sigma > 0$, and a shape parameter ξ in $\mathbb{R}$. It is defined as:

$$F_X(x) = 1 - \left\{1 + \xi\left(\frac{x-\mu}{\sigma}\right)\right\}^{-\frac{1}{\xi}} \quad \xi \neq 0, \quad (3)$$

where x is larger than a threshold μ. On the other hand, the GEV uses the same parameters and is expressed as:

$$F_Y(y) = \exp\left[-\left\{1 + \xi\left(\frac{y-\mu}{\sigma}\right)\right\}^{-\frac{1}{\xi}}\right] \quad \xi \neq 0 \quad (4)$$

with domain $1 + \xi\left(\frac{y-\mu}{\sigma}\right) > 0$ for $\xi \neq 0$. In the limiting case of $\xi = 0$, the GEV distribution corresponds to the Gumbel distribution. The GPD and GEV were chosen because of their good fit to the data tested with the Kolmogorov–Smirnov, Anderson–Darling, and upper-tail Anderson–Darling goodness-of-fit tests;

9. Computation of the duration of the design event (D_T) by $D_T = f(t_p) \cdot V_T/Q_T$, where $f(t_p)$ is the lognormal density at the time of peak t_p;
10. Composition of the design hydrograph using the hydrograph shape given by the PDF ($f(t)$), the design

variable quantiles (V_T and D_T), and the baseflow (B) as described by:

$$Q_T(t) = f(t)V_T/D_T + B. \quad (5)$$

For a detailed description of the methodology, the reader is referred to Brunner et al. (2017b). We applied this method to construct hydrographs for a return period of 100 years, which is frequently used in hydraulic design in Switzerland (Camezind-Wildi 2005). The design flood hydrographs obtained using this method are composed of ten parameters (Fig. 2), which we herein refer to as *SDH parameters*. Two of the parameters are related to the hydrograph shape and therefore to the time evolution of the event while eight of the parameters are related to the hydrograph magnitude. The hydrograph shape is defined by the lognormal PDF with a location and a scale parameter. The marginal distributions of the design variables (peak discharges and hydrograph volumes) are modeled by three parameters each (location, scale, and shape). One parameter defines the dependence between these two variables (θ) and one parameter characterizes the proportion of baseflow to be added to the direct runoff hydrograph (I_{BF}). The statistics of the ten SDH parameters for all study catchments are summarized in Table 1.

Some of the parameters can be assumed normally distributed (see histograms in Fig. 3), which was confirmed by the Shapiro–Wilks goodness-of-fit test (Shapiro and Wilk 1965). However, the location and scale parameters of the marginal distributions of the peak discharges (GPD) and the hydrograph volumes (GEV) are skewed to the right. The location and the scale parameter of the GPD and the GEV distribution are strictly positive (Coles 2001). Some of the SDH parameters are correlated with other SDH parameters (see scatterplots and Kendall's correlation coefficients in Fig. 3). The two parameters of the PDF are negatively correlated while the location and scale parameters of the marginal distributions GEV and GPD are positively correlated. The shape parameters of the marginal distributions of the design variables, the baseflow index (I_{BF}), and the dependence parameter (θ) can be considered as independent of the other SDH parameters since their correlation to other SDH parameters is very weak.

The scale and shape parameters of the probability density function used to fit the runoff hydrograph are

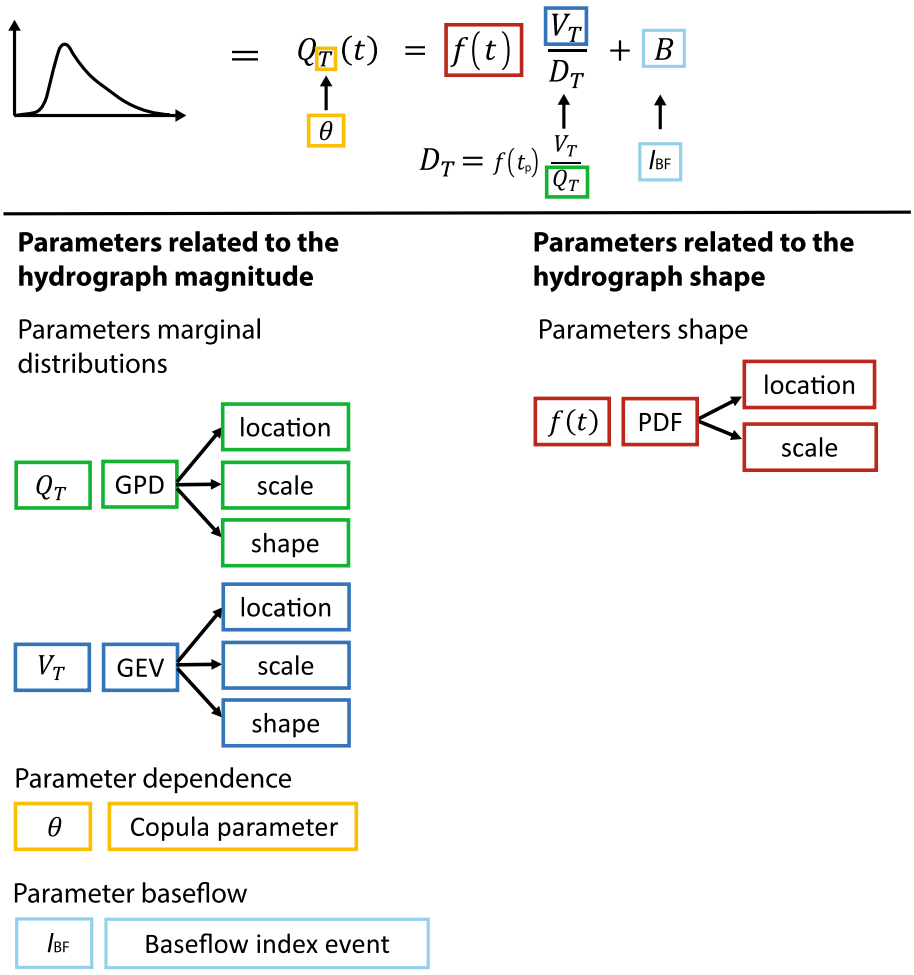

Fig. 2 Overview of the parameters involved in the construction of an SDH. $Q_T(t)$ can be expressed as the product of the value of a PDF f at the time of the peak t_p and the quotient of the hydrograph volume estimated for a return period V_T and the duration of the event estimated for a return period D_T. The baseflow (B) is then added to the directflow (top panel). The ten parameters needed for the construction of SDHs are presented in the bottom panel and are: Location and scale parameter of the PDF (red), parameters of the marginal distribution of the hydrograph volumes (blue), parameters of the marginal distribution of the peak discharges (green), copula parameter (yellow), and baseflow index event (light blue). The location and scale parameter of the PDF are related to the hydrograph shape while the other eight parameters are related to the hydrograph magnitude

Table 1 Summary statistics of the ten SDH parameters over all study catchments

SDH parameter	Mean	Standard deviation	Coefficient of variation	Unit
I_{BF}	0.45	0.13	0.29	–
PDF location	− 0.95	0.21	− 0.22	–
PDF scale	0.58	0.141	0.24	–
GPD location	13.48	28.56	2.12	m^3/s
GPD scale	14.31	25.76	1.80	m^3/s
GPD shape	− 0.05	0.15	− 3.16	–
GEV location	1.22	2.41	1.98	Mm^3
GEV scale	0.42	0.77	1.84	Mm^3
GEV shape	0.18	0.11	0.62	–
θ	1.88	0.43	0.23	–

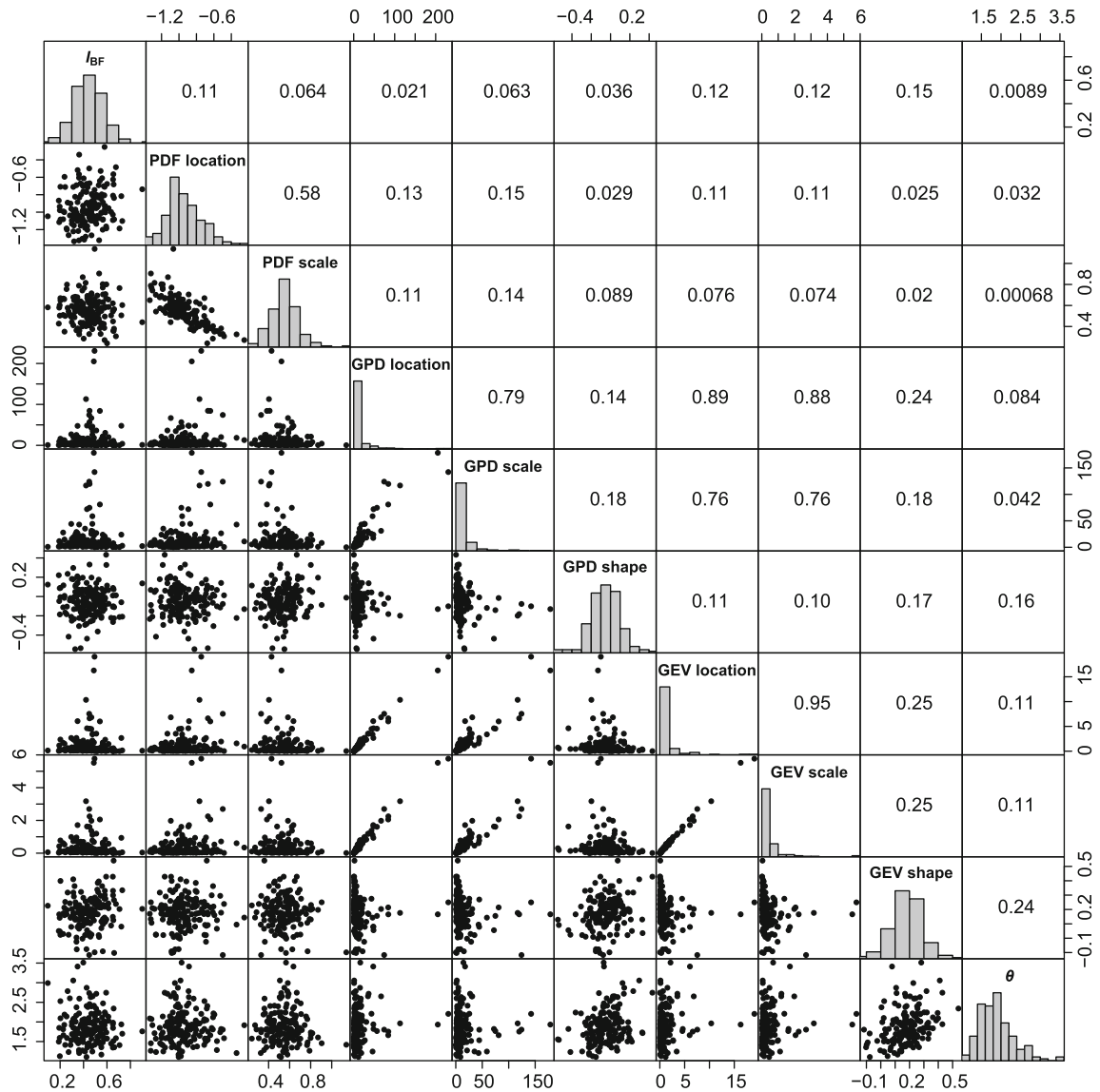

Fig. 3 Histograms of the different SDH characteristics (diagonal), scatterplots of the SDH parameters in relation to the others (lower left panel), and Kendall's correlation coefficients between the different SDH parameters (upper right panel)

dependent. Similarly, the location, scale, and shape parameters of the GEV and the GPD are dependent on each other. Nonetheless, in the first step, these dependencies were neglected and each SDH parameter was regionalized separately. In the second step, we considered these dependencies, if allowed for by the regionalization method. Namely, multivariate regression and the methods based on the transfer of the whole parameter set from homogeneous regions, account for these dependencies.

2.3 Auxiliary variables

To predict runoff or runoff-related variables, such as the parameters of an SDH, in catchments without runoff measurements, alternative information has to be used (Blöschl et al. 2013) which ideally characterizes the factors that drive the hydrological response of a catchment.

Catchment characteristics We used a set of catchment characteristics that have been used and proven to be useful in previous regionalization studies (for a synthesis on the use of different catchment characteristics see (He et al. 2011)). Most characteristics were computed using the PREVAH pre-processing tool WINHRU (Viviroli et al. 2009b). WINHRU derived physiographical characteristics from the digital elevation model (DEM), landuse related characteristics from digital maps of landuse (Bundesamt für Statistik 2003), soil related characteristics from digital maps of land surface characteristics (Eidgenössishe Forshungsanstalt für Wald Shnee und Landshaft 1999), hydrogeology related characteristics from a map that focuses on groundwater resources (Bitterli et al. 2007), and geology related attributes from the Swiss geotechnical map (Bundesamt für Statistik 2003). For a detailed description of the computation procedure, we refer the reader to Viviroli et al. (2009a). The climatological characteristics were computed based on tables from the Hydrological Atlas of Switzerland (Jensen et al. 1997) and on gridded meteorological data provided by MeteoSwiss (MeteoSwiss 2013). The population density was computed based on a population map for Switzerland (Bundesamt für Statistik 2003).

The final set of 54 catchment characteristics (Table 2) consists of features related to the geographical location of the catchment centroid (2 characteristics), the physiography of the catchment (13), landuse (6), soil properties (6), hydrogeology (9), geology (6), climate (11), and population (1). These catchment characteristics form a solid basis for the regionalization analysis. However, some of the explanatory variables are highly correlated and contain redundant information. The potential of single catchment characteristics for aiding regionalization is indicated by an assessment of their linear relationship with the individual SDH parameters. Some SDH parameters (baseflow index (I_{BF}), the location and scale parameter of the marginal distributions of Q_p and V, and the dependence parameter θ) show Pearson's correlation coefficients higher than 0.4 with some of the catchment characteristics. However, the location and scale parameter of the PDF and the shape parameters of the marginal distributions of Q_p and V are only weakly correlated to the catchment characteristics.

Spatial information In addition to the characteristics mentioned above, the location of the catchments in space can be relevant for the spatial regionalization methods (see methods colored in red in Fig. 4). The coordinates of the gauging stations were used for kriging methods and a shape file for each catchment for the topological kriging methods. Linear and nonlinear approaches as well as methods based on the building of homogeneous regions use the information provided by the catchment characteristics while spatial methods use spatial information.

3 Methods

3.1 Overview

We tested several methods (Fig. 4) that have been described in hydrological and statistical literature. Testing all these methods allowed us to find the most appropriate method for the transfer of design hydrograph parameters to ungauged catchments. We grouped regionalization methods, in a similar way as other authors (e.g. Steinschneider et al. 2014), into three main classes: (1) methods based on the relation between catchment characteristics and model parameters, (2) approaches based on spatial proximity, and (3) methods based on homogeneous regions.

We followed two main strategies to regionalize the SDH parameters: (1) we regionalized each parameter individually and (2) we regionalized the ten SDH parameters (see Figs. 2, 3) as a set to assure that the relation between the parameters was not disturbed (Bardossy 2007; Parajka et al. 2005; Viviroli et al. 2009a). The individual parameters were regionalized using methods based on the relationship between catchment characteristics and model parameters, approaches based on spatial proximity, and regional mean models. On the other hand, the set of SDH parameters was regionalized using methods based on homogeneous regions. Figure 4 shows which methods were tested for the regionalization of the individual parameters and which methods were tested for the regionalization of the entire parameter set. Most models for the individual parameters were fitted on a *global* scale using data from all 163 study catchments. In addition, we fitted regional mean models for each parameter. The

Table 2 Catchment characteristics available for regionalization and their description

Class	Catchment characteristic	Description
Location	X Coordinate of catchment centroid for regression methods and of catchment outlet for kriging methods	West-East position in Swiss uniform map projection grid
	Y Coordinate of catchment centroid for regression methods and of catchment outlet for kriging methods	South-North position in Swiss uniform map projection grid
Physiography	Catchment area	–
	Mean altitude	–
	North exposed surfaces	Percentage of area exposed to the North
	East exposed surfaces	Percentage of area exposed to the East
	South exposed surfaces	Percentage of area exposed to the South
	West exposed surfaces	Percentage of area exposed to the West
	Shape parameter 1	Area / (distance between catchment center and the most remote point)^2
	Shape parameter 2	Length main channel / length of main channel down to the catchment center
	Inclination	Percentage of surfaces with inclination $<3^\circ$
	Relief energy	Maximum elevation -minimum elevation
	Length of main channel	–
	Network density	Length of main channel / area
	Slope of main channel	–
Landuse	Pastures and arable land	Percentage area with pastures and arable land
	Settlements	Percentage area with settlements
	Forest	Percentage of forested areas
	Glaciers	Percentage of areas with glaciers
	Contributing areas	Percentage or areas with a distance of 250 m to the channel
	Soil	Percentage of soil-covered areas
Soil	Hydraulic conductivity, average	Based on 100×100 m^2 gridded data
	Hydraulic conductivity, skewness	Based on 100×100 m^2 gridded data
	Net field capacity, standard deviation	Based on 100×100 m^2 gridded data
	Net field capacity, skewness	Based on 100×100 m^2 gridded data
	Soil topographic index, standard deviation	Based on 100×100 m^2 gridded data
	Soil topographic index, skewness	Based on 100×100 m^2 gridded data
Hydrogeology (groundwater)	Percentage area of unconsolidated rock, high permeability	Mainly well-porous gravel in alluvial valleys
	Percentage area of unconsolidated rock, intermediate permeability	Porous gravel, sandy gravel, medium-to coarse-grained debris
	Percentage area of unconsolidated rock, low permeability	Silty gravel, fine-to medium-grained debris, moraines
	Percentage area of unconsolidated rock, impermeable	Clay, silt, fine sand, loamy moraines
	Percentage area of hard rock, generic	Fractured-porous rock
	Percentage area of hard rock, impermeable	Marl, mudstone, shale, gneiss, well-cemented sandstone
	Percentage area of karstic rock	Carbonate and sulfate rock
	Hydraulic topographic index, standard deviation	Based on 100×100 m^2 gridded data
	Hydraulic topographic index, skewness	Based on 100×100m^2 gridded data
Geology (geotechnics)	Percentage area of hard rock, permeable	Various kinds of hard rock with pores, fissures, or karst
	Percentage area of hard rock, variable permeability	Marl, sandstone
	Percentage area of hard rock, impermeable	Marl, shale, clay, argillaceous slate, phyllite
	Percentage area of unconsolidated rock, low permeability	Clayey silts and clay

Table 2 Catchment characteristics available for regionalization and their description

Class	Catchment characteristic	Description
	Percentage area of unconsolidated rock, variable permeability	Sands and silts, debris
	Percentage area of unconsolidated rock, high permeability	Gravel and sands
Climate	Hourly precipitation, average	Based on precipitation values $\geq$ 0.1 mm/h
	Hourly precipitation, coefficient of variation	Based on precipitation values $\geq$ 0.1 mm/h
	Hourly precipitation, seasonality	Average day of the year of occurrence
	Hourly precipitation, variability of seasonality	Variability of the day of the year
	Maximum precipitation intensity during 1 h	Return period 2.33 years
	Maximum precipitation intensity during 24 h	Return period 2.33 years
	Maximum precipitation intensity during 24 h	Average date of occurrence
	Maximum precipitation intensity	–
	Maximum precipitation intensity / Maximum precipitation intensity during 1 h	–
	Average annual vapor pressure	–
	Average annual sunshine duration	Percentage of maximum possible sunshine duration
Population	Population density	Number of inhabitants per area
Total		54

models for the regionalization of the entire parameter set were established on a regional scale and only consider a subset of these 163 study catchments. The methods tested to regionalize the ten SDH parameters are listed and shortly described below. They were implemented in *R* (R Core Team 2015) and technical details are provided in Table 3. We refer the reader to Harrell (2015) for a more detailed descriptions of linear regression methods, to Harrell (2015) or James et al. (2013) for a description of nonlinear regression methods, and to Webster and Oliver (2007) for more details on spatial methods.

3.2 Methods based on the relation between catchment characteristics and model parameters

A relationship was established between catchment characteristics and model parameters from the information available in gauged catchments. This relationship was assumed to be equally valid in ungauged catchments within the study region, which allowed for the estimation of model parameters from catchment characteristics. The models belonging to this class are linear and nonlinear regression models. Linear regression models only consider the linear relationship between catchment characteristics and model parameters. In contrast, nonlinear regression models such as regression trees also take into account nonlinear relationships between catchment characteristics and model parameters (Ji et al. 2013; Takezawa 2012).

3.2.1 Linear regression methods

We used ten multiple regression equations to express each of the SDH parameters (response variable) as a function of some catchment characteristics (explanatory variables). The regression parameters were estimated from the computed SDH parameters and the computed catchment characteristics using a least squares approach (Rosbjerg et al. 2013). As mentioned in Sect. 2, some of the SDH parameters had to be strictly positive. However, regression methods do typically not restrict prediction to strictly positive values. We followed two strategies to guarantee strictly positive values when predicting the location and scale parameters of the GPD and the GEV distribution. We worked on the log-transformed data if this guaranteed positive predictions. If not, we fitted a Gamma generalized linear model with a log-link, which does not give rise to a negative estimated response (Myers et al. 2010). For simplicity, we will refer to the linear regression models and to the Gamma generalized linear model as linear models.

Full regression First, we fitted a multiple regression model to the data which used all the 54 available catchment characteristics as explanatory variables. The full regression model had the disadvantage that multicollinearity was present in the set of explanatory variables, i.e., the explanatory variables were highly correlated with each other (James et al. 2013). To alleviate the problem of multicollinearity, we tested several methods that choose a subset of explanatory variables to be included in the regression model (see e.g., Harrell 2015; James et al.

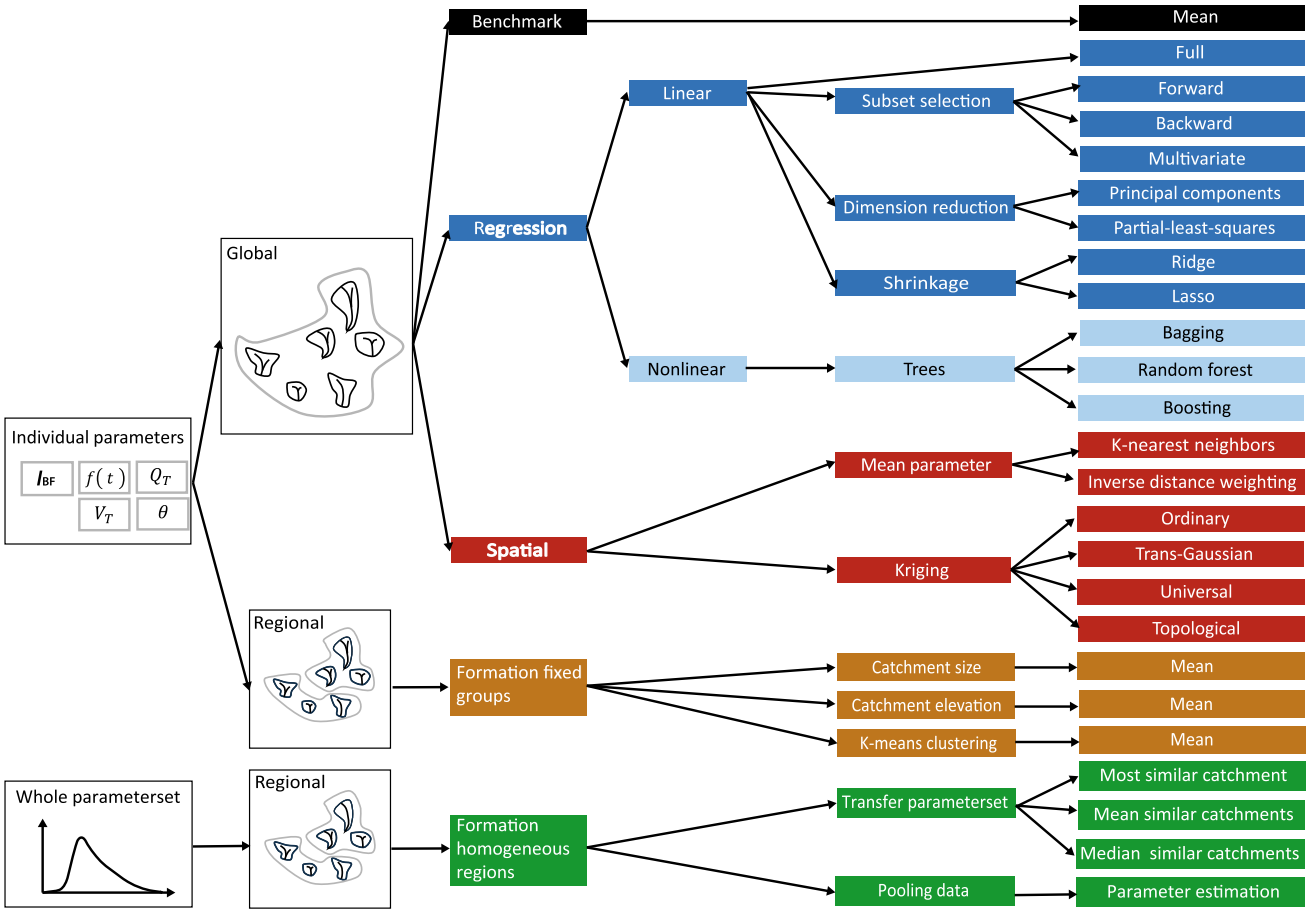

Fig. 4 Overview of the methods tested to regionalize the ten SDH parameters on a global or regional scale. The methods were grouped into benchmark (black), regression (blue), and spatial (red) models, plus models based on the formation of regions using catchment characteristics (brown and green)

Table 3 Technical details for the methods used in this study

Method category	Method	R package	Functions
Linear regression	Full	*stats* (R Core Team 2015)	*lm* and *glm*
	Subset selection	*stats* (R Core Team 2015)	*step*
	Dimension reduction	*pls* (Mevik and Wehrens 2007)	*pcr* and *plsr*
	Shrinkage	*glmnet* (Friedman et al. 2010)	*glmnet*
	Multivariate	*stats* (R Core Team 2015)	*lm*
Nonlinear regression	Bagging	*ipred* (Peters et al. 2015)	*bagging*
	Random forest	*randomForest* (Liaw and Wiener 2002)	*randomForest*
	Boosting	*gbm* (Ridgeway 2007)	*gbm*
Spatial approaches	Mean parameter	*FNN* (Beygelzimer et al. 2013)	*get.knn*
	Kriging	*gstat* (Pebesma 2004)	*fit.variogram* and *krige*
	Topological kriging	*rtop* (Skoien et al. 2014)	*rtopFitVariogram* and *rtopKrige*

2013). These can be summarized as subset selection, dimension reduction, and shrinkage techniques.

Subset selection Subset selection involved the identification of a subset of the 54 catchment characteristics that were most strongly related to the SDH parameters. A model was then fitted using this reduced set of variables. We applied stepwise forward and backward selection to

find a regression model with a reduced set of explanatory variables (Harrell 2015).

Dimension reduction We applied principal components regression (PCR) and partial-least-squares (PLS) regression (Harrell 2015; James et al. 2013; Kiers and Smilde 2007) to explain the SDH parameters by a reduced number of variables. Both methods projected the 54 explanatory variables into a smaller m-dimensional subspace. The regression models were then fitted using the new m explanatory variables. In PCR, the regression is a linear combination of all the original explanatory variables. PLS regression is an alternative to PCR which uses not only the explanatory variables to form linear combinations but also the SDH parameters.

Shrinkage We used ridge regression (Le Cessie and van Houwelingen 1992) and lasso (Tibshirani 1997) to fit a model using all p explanatory variables. However, the estimated regression parameters were shrunk towards zero relative to their least squares estimates. While ridge regression included all p explanatory variables in the final model, the lasso shrank some of the model parameter estimates exactly to zero and therefore performed variable selection (Harrell 2015; James et al. 2013).

Multivariate regression The methods presented above fitted one regression equation per SDH parameter and neglected that some of the SDH parameters are correlated. Multivariate regression (or regression with multiple equations), as opposed to multiple regression, considers that some of the SDH parameters are correlated (Tung et al. 1997). We used generalized least squares (GLS) estimation, which required a covariance matrix for the errors, instead of ordinary least squares (OLS) (Weisberg 2005) to estimate the regression parameters of the multivariate regression system. The least squares residuals of the individual regression equations for each SDH parameter gave an idea of the error covariances and were used to estimate the elements of the error covariance matrix (Greene 2002). However, OLS and GLS were identical when the SDH parameters considered were uncorrelated and when all the regression equations had identical explanatory variables (Greene 2002). We therefore defined an individual subset of catchment characteristics chosen by stepwise forward selection for each SDH parameter to be used by the multivariate regression and only applied multivariate regression to those SDH parameters that were highly correlated (GEV location and scale and GPD location and scale) (see Kendall's correlation coefficients in Fig. 3). The regression parameters of the multivariate regression system were estimated using GLS. The GLS is the method to be used to fulfill all the theoretical assumptions, however, the prediction outcome is not significantly different from applying OLS on equation-by-equation regression because both OLS and GLS estimates are unbiased.

3.2.2 Nonlinear regression methods

We applied three types of tree-based techniques which combine a large number of trees into an ensemble (Strobl et al. 2009): bagging, random forest, and boosting.

Bagging We applied bootstrap aggregation to reduce the variance and increase the prediction accuracy of regression trees (Liaw and Wiener 2002; Breiman 1996). The predictions were obtained by averaging the predictions obtained by several prediction models built based on bootstrapped samples.

Random forest We used random forest to decorrelate the regression trees built on several bootstrapped samples. Each split only considered a subset of the explanatory variables.

Boosting Boosted regression trees were used to build successive trees in a stagewise procedure where new trees depended on previous trees. Only a proportion of the observations was selected at each step to fit the tree model to prevent from overfitting.

In addition to the nonlinear approaches described above, other nonlinear methods were proposed in the literature to estimate hydrological parameters or flood quantiles for ungauged catchments. For example, Abrahart and See (2007), Aziz et al. (2015, 2016), Dawson et al. (2006), and Shu and Ouarda (2008) applied artificial neural networks (ANNs) that can be trained to represent the relationship between a range of catchment descriptors and associated hydrological parameters. However, ANNs do not allow for the determination of the role of individual variables, which reduces the confidence in model predictions (Dawson et al. 2006). They were therefore excluded from this analysis.

3.3 Approaches based on spatial proximity

This second class of methods is based on the assumption that the model parameters are more similar for catchments closer in a geographical or physiographical space than for catchments further apart (Rosbjerg et al. 2013). Nearly all spatial prediction methods, including the simpler forms of kriging, can be seen as weighted averages of data. Methods that are frequently used to interpolate data and use a weighted average of data from measured locations are nearest neighbor(s), inverse distance weighting, and kriging (Webster and Oliver 2007).

3.3.1 Mean parameter

Nearest neighbors We determined the five nearest neighbors for each station in terms of the Euclidean distance and computed the mean of the different SDH parameters which then served as the predictions for the station under consideration (Parajka et al. 2005; Viviroli et al. 2009a). We

chose five neighbors as a compromise between including more information and defining non-similar catchments as nearest neighbors.

Inverse distance weighting of nearest neighbors We used again the five nearest neighbors of a station and gave their observations weights according to the inverse Euclidean distance from the prediction point (Hechenbichler and Schliep 2004; Lu and Wong 2008; Samuel et al. 2011). The predicted values were a weighted average of the observations at the neighboring stations.

3.3.2 Kriging

In addition to the classical interpolation methods described above, we applied several kriging approaches, which consider the value observed at one point as a realisation of a spatial process (Matheron 1971). Kriging is based on the concept that values at locations near to one another are similar, whereas those at more distant locations are less correlated. This dependence structure is typically characterized by a variogram. In order to perform kriging, several steps are necessary: first, the empirical variogram is computed, second a theoretical model is fitted to this empirical variogram, then, the fitted variogram model is used to calculate the kriging weights by solving a system of equations, and finally, interpolation is carried out. The kriging methods tested differ in the assumptions about the mean structure of the model. We estimated the variograms based on the spatial information and used them for kriging. However, variograms could theoretically also be based on a physiographical space constructed using physiographical and meteorological characteristics of gauging stations and multivariate analysis techniques, such as canonical correlation analysis (CCA) or principal components analysis (PCA) (Archfield et al. 2013; Castiglioni et al. 2011; Chokmani and Ouarda 2004; Hundecha et al. 2008; Ouarda et al. 2000). In our case, many principal components or canonical variables were needed to explain an acceptable proportion of the total variance.

Ordinary kriging Ordinary kriging assumes that the mean of the model system is unknown but constant and that the data is symmetrically distributed. We computed the empirical variogram for all SDH parameters among which not all showed a structure (i.e., PDF location and scale showed no structure). A classical exponential variogram was fitted to the empirical variogram.

Trans-Gaussian kriging A symmetric distribution as assumed for ordinary kriging did not describe the behavior of all the data analyzed. One of the simplest ways to extend the symmetric model is to assume that the model holds after applying a transformation of the original data. We did trans-Gaussian kriging on the log-transformed data (Diggle and Ribeiro Jr 2007; Yamamoto 2007) for those parameters that were not normally and therefore symmetrically distributed (see Fig. 3). The kriging estimates obtained by lognormal kriging had to be back transformed to the original measurement scale by taking the exponential of the kriging estimates plus correcting the bias (Yamamoto 2007). The log-transformation was only possible for positive values (Osborne 2010).

Universal kriging We used universal kriging to model the spatial trend using catchment size as the explanatory variable (Bardossy and Lehmann 1997; Merz and Blöschl 2004). The variogram was computed from the residuals obtained after having removed the linear trend due to catchment size. We also tested elevation and a combination of five catchment characteristics found to be important in multiple regression as explanatory variables. However, these options led to a clearly worse performance than when using catchment area and were therefore not followed up on.

Topological kriging We finally used topological kriging (Skoien et al. 2006) to estimate the SDH parameters in ungauged catchments. Unlike ordinary kriging, it takes both the area and the nested nature of catchments into account (Gottschalk 1993; Gottschalk et al. 2011; Sauquet 2006).

3.4 Methods based on homogeneous regions

This third class of methods assumes that hydrologically homogeneous regions can be found based on catchment characteristics (Burn and Boorman 1992; Prinzio et al. 2011). We formed homogeneous regions in a physiographical space defined by catchment characteristics (Castiglioni et al. 2011; Chokmani and Ouarda 2004). In a first step, we divided the space into fixed regions (GREHYS 1996). In a second step, we formed regions of influence (Burn 1990) for each catchment separately.

3.4.1 Regional mean models

We formed three regions of approximately equal size (50 catchments) that still contained enough catchments to fit a region specific regression model (Burn and Boorman 1992; Laaha et al. 2014; Ouarda et al. 2001). The regions were formed using two catchment characteristics that are considered to be hydrologically meaningful: catchment size and mean elevation. The three size zones were defined as catchments smaller than 30 km^2, catchments with sizes between 30 and 90 km^2, and catchments larger than 90 km^2. The three elevation zones defined were catchments lower than 600 m.a.s.l., catchments between 600 and 850 m.a.s.l., and catchments higher than 850 m.a.s.l.. These regions were used to compute the arithmetic mean (Razavi and Coulibaly 2013) and to fit regression models on the

regional scale (Nathan and McMahon 1990; Salinas et al. 2013; Sauquet and Catalogne 2011). We focused on the regional mean model since our preliminary analysis showed that regression models did not perform better on a regional than on a global scale as supported by Kjeldsen and Jones (2010) but in contrast to findings by Salinas et al. (2013) and Sauquet and Catalogne (2011). The minimum sample size to compute the arithmetic mean is much smaller than the sample size required for fitting a reliable regression model. Therefore, the number of regions could be increased. We used *k*-means clustering (Halkidi et al. 2001) to form homogeneous regions in terms of catchment characteristics (Burn 1989; Burn and Boorman 1992), which were standardized by their standard deviation over all catchments (Burn and Boorman 1993). The predictive performance of the model increased with an increase in the number of regions. However, we divided the catchments into only ten regions in order to not reduce the number of catchments per group too much, which might result in an overfitting of the model. The arithmetic mean was also computed for the regions obtained by 10-means clustering.

3.4.2 Transfer from similar catchments

We first formed homogeneous regions and then transferred the parameter sets using different techniques for the transfer of the entire parameter set from similar catchments to the catchment under consideration.

Formation of homogeneous regions The entire set of parameters was regionalized based on the formation of regions, where each basin has its own region (Acreman and Sinclair 1986; Burn 1990) consisting of similar catchments. Similarity was defined by the Euclidean distance in the catchment characteristics space (Burn 1990; Burn and Boorman 1992; Rasmussen et al. 1993) where the catchment characteristics were normalized by their standard deviation across the whole catchment set (Oudin et al. 2010). Flood statistics were excluded from the analysis because they are not available for ungauged catchments (Ilorme and Griffis 2013). The catchment characteristics used to span the space were obtained using three different techniques since all methods for determining homogeneous regions require subjective choices (GREHYS 1996; Ilorme and Griffis 2013):

1. Hydrological reasoning (Ouarda et al. 2000): Selection of six catchment characteristics that are supposed to be hydrologically meaningful: catchment area, mean catchment elevation, network density, mean annual rainfall, and *X*-and *Y*-coordinates.
2. Best-*H*: Random set of catchment characteristics leading to the lowest mean *H*-statistic, a homogeneity measure proposed by Hosking and Wallis (1993), for the regions obtained for the different catchments. This set consists of the following catchment characteristics: proportion of south exposed areas in the catchment, length of the main channel, percentage of area covered by hard rock, percentage of surfaces with inclination smaller than three degrees, and maximum 24h-precipitation.
3. CCA: Set of catchment characteristics obtained by canonical correlation analysis (CCA) between the catchment characteristics and the *L*-moments of peak discharges and hydrograph volumes (Cavadias et al. 2001; He et al. 2011; Ouarda et al. 2000, 2001). This set consists of the following catchment characteristics: average precipitation, maximum precipitation intensity over a time interval of 1 h, percentage of contributing areas, network density, percentage of area covered by hard rock, *X*-and *Y*-coordinate, hourly precipitation variability, percentage of surfaces with inclination smaller than three degrees, population density, percentage of area covered by unconsolidated rock, percentage of soil covered areas, percentage of sealed areas, and percentage of agricultural areas.

Based on the distance matrices, the most similar catchments were identified for each target catchment. We used the five most similar catchments because this number optimized the predictive performance over all SDH parameters and has already been found appropriate in previous studies (Viviroli et al. 2009a). Still, the homogeneity in terms of Hosking and Wallis' *H*-statistic was not good. Only 26% of the regions formed could be said to be homogeneous in terms of peak discharge (looking at its *L*-moments), which is not surprising since there is often a lack of correlation between catchment descriptors and flow-derived characteristics (Ali et al. 2012).

Transfer methods Despite this lacking hydrological homogeneity, we transferred the SDH parameter set from the formed regions to the target catchment using the following four strategies:

1. Transfer of the parameter set from the most similar catchment adjusted by the catchment size (Parajka et al. 2005; Zhang and Chiew 2009);
2. Transfer of the mean parameter set of the five most similar catchments adjusted by the catchment size (Oudin et al. 2008). We chose the five most similar catchments since this can average out the effect of choosing a poor donor catchment and most studies use between five and ten catchments for averaging (Zhang and Chiew 2009). Averaging the parameters resulted in much more plausible results than averaging the output of the five models;
3. Transfer of the median parameter set of the five most similar catchments adjusted by the catchment size. The median set is expected to reduce the influence of a

catchment having rather different SDH parameters than the other catchments compared to the mean set;
4. Estimation of a new parameter set based on the pooled runoff data from the five most similar catchments. Data pooling increases the size of the data set (Ilorme and Griffis 2013) which can be especially advantageous when estimating the parameters of the distribution of extremes (Castellarin et al. 2001; Gaál et al. 2008).

3.5 Benchmark model

To compare the predictive performances of the regionalization methods tested, we used the arithmetic mean of the individual SDH parameters as a simple benchmark model (Parajka et al. 2005; Razavi and Coulibaly 2013; Steinschneider et al. 2014).

3.6 Model validation

We used k-fold cross validation to validate the performance of the regionalization methods tested. The data was divided into 10 parts, also called folds, of equal size. The model parameters were estimated based on 10 minus 1 folds, and the model was validated on the remaining fold. This procedure was repeated for each fold in turn (Hastie et al. 2008; James et al. 2013).

To validate the methods, we compared on the one hand the regionalized or predicted SDH parameters to the SDH parameters estimated based on runoff data. On the other hand, we compared the hydrograph resulting from the regionalized SDH parameters to the SDH estimated based on runoff observations. Complementing the validation of the hydrograph characteristics with a validation of the single parameters allows for a better understanding of why a given approach outperforms the other (Steinschneider et al. 2014). The performance of the different regionalization methods in terms of the individual SDH parameters can be assessed using different measures such as the bias (deviation in the mean), the mean squared error (E_{MS}), the root mean squared error (E_{RMS}), or the (absolute) relative error (Chebana and Ouarda 2009; Ouarda et al. 2006; Salinas et al. 2013; Shu and Ouarda 2008). Here, we used the absolute relative error (E_{AR}) and the mean absolute relative error (E_{MAR}) because they allow us to compare the performance of the different regionalization methods to the performance of the benchmark model. Further, they allow a comparison of how well the different SDH parameters can be predicted. E_{AR} and E_{MAR} (Sauquet 2006) are given by

$$E_{\mathrm{AR}} = \left| \frac{X_{ic} - X_{ir}}{X_{ic}} \right| \tag{6}$$

and

$$E_{\mathrm{MAR}} = \frac{1}{n} \sum_{i=1}^{n} \left| \frac{X_{ic} - X_{ir}}{X_{ic}} \right|, \tag{7}$$

where X_{ic} is the computed SDH parameter or characteristic, X_{ir} is the regionalized parameter or SDH characteristic, and n is the number of catchments in the data set.

When looking at the predictive performance in terms of the whole hydrograph, one single goodness-of-fit criterion is usually not sufficient to assess the fit between a constructed and a regionalized hydrograph (Green and Stephenson 1986). Therefore, Green and Stephenson (1986) recommended to compute the relative error of individual hydrograph characteristics such as peak discharge (Q_{p}) and volume (V) between the regionalized and the constructed hydrograph. In addition, we also assessed the error of the hydrograph shape via the relative error of the time to peak (t_{p}) (Tung et al. 1997) and the time between the peak and where the recession reaches half of the peak discharge (t_{p05}). We will refer to t_{p05} as *half-recession time* (see Fig. 5 for an illustration of the different hydrograph characteristics).

3.7 Importance of catchment characteristics

Several of the tested regionalization methods allow us to identify catchment characteristics that were important to explain the SDH parameters via a variance importance plot. Namely, these approaches are the subset selection techniques (forward and backward), the shrinkage technique lasso, the dimension reduction techniques principal components-and partial-least squares regression, bagged regression trees, random forest, and boosted regression trees. We identified the five most important catchment characteristics in each of these approaches. Catchment characteristics that are important in at least four out of the eight approaches were said to be important for the prediction of the SDH parameter under consideration.

4 Results

4.1 Validation of the individual SDH parameters

Figure 6 shows the E_{MAR} of the ten SDH parameters for the regionalization methods that were used to regionalize the individual parameters comprising the benchmark model, linear regression models, nonlinear regression models, spatial models, and regional mean models (see Fig. 4). Our results show that we can find a better model than the benchmark model for the regionalization of most SDH parameters (I_{BF}; GPD location, scale, and shape; GEV location, scale, and shape; and θ). However, this is not

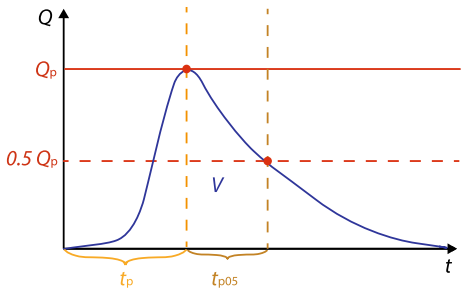

Fig. 5 Illustration of the hydrograph characteristics used for the validation of the regionalization methods: peak discharge (Q_p), hydrograph volume (V), time to peak (t_p), and half-recession time (t_{p05})

possible for those SDH parameters describing the hydrograph shape (PDF location and scale). This implies that working with a simple mean value for the PDF parameters is sufficient and working with a more complex model does not lead to improved results. In general, nonlinear regression techniques (especially boosting) perform slightly better than linear regression techniques. For some parameters (I_{BF}, GPD shape, and θ), spatial methods perfom better than linear regression methods. For others (GPD location and scale and GEV location and scale) linear regression methods perform better than spatial methods (except for universal kriging where a linear component is included in the model). The regional mean models generally perform better than the global mean model (benchmark). E_{MAR} varies significantly across SDH parameters. On the one hand, the parameter I_{BF} and the two PDF parameters show low E_{MAR} (i.e. good performance) over all regionalization methods including the benchmark model. On the other hand, the SDH parameters related to the magnitude of the event (GEV location, scale, and shape and GPD location, scale, and shape) show relatively high E_{MAR} (i.e. bad performance) for some methods.

4.2 Validation of the whole design hydrograph

The predictive performance of the whole hydrograph (for an example see Fig. 7) is displayed in Fig. 8. It is represented by

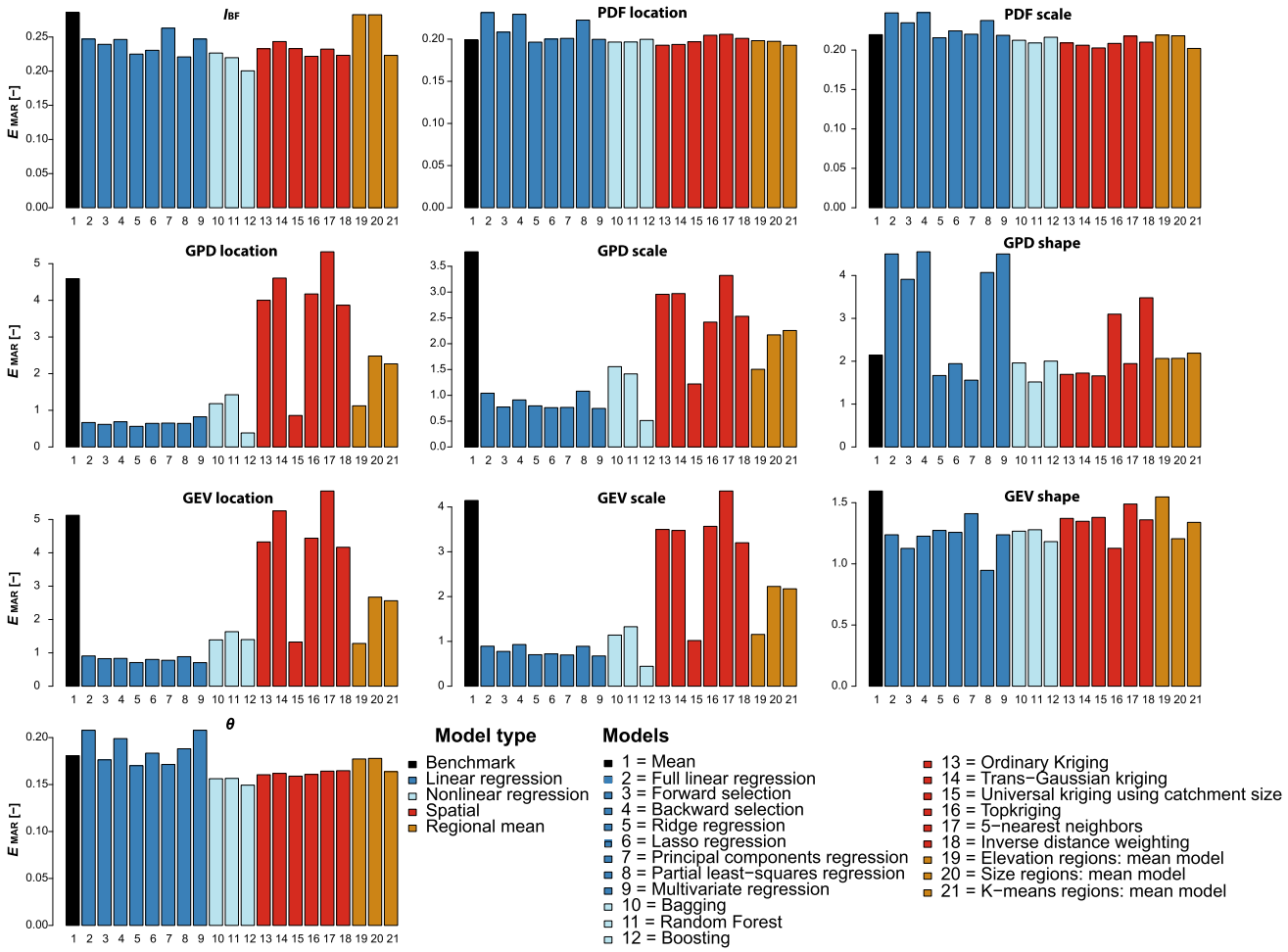

Fig. 6 Predictive performance of the different regionalization methods (black: benchmark, blue: linear regression, light blue: nonlinear regression, red: spatial, brown: regional mean models) in terms of the mean absolute relative error (E_{MAR}) for the ten SDH parameters

boxplots of the E_{AR} for the different catchments for the four different hydrograph characteristics Q_p, V, t_p, and t_{p05} (see Fig. 5). The predictive performance for Q_p (Fig. 8a) and V (Fig. 8b) is significantly better for linear and nonlinear regression techniques and when transferring the entire parameter set based on the formation of homogeneous regions (using the strategy of hydrological reasoning) than for the benchmark model. However, when looking at the hydrograph shape represented by the time to peak and the half-recession time (Figs. 8c and d), no model can be found that better regionalizes the shape than the benchmark model. The E_{AR} are generally higher for the magnitude of the event (Q_p and V) than for the shape of the event (t_p, t_{p05}). The E_{AR} of the temporal hydrograph characteristics t_p and t_{p05} are not correlated to the E_{AR} of the magnitude of the event characterized by Q_p and V. This means that a model badly predicting the shape of the event does not necessarily badly predict the magnitude of the event and *vice versa*. However, the performance of the two characteristics Q_p and V is closely linked (Kendall's correlation coefficient > 0.6).

4.2.1 Regionalization based on the formation of homogeneous regions

The predictive performance of the regionalization methods based on the formation of homogeneous regions in terms of the four hydrograph characteristics Q_p, V, t_p, and t_{p05} can not be improved by applying a different distance metric than the one based on hydrological reasoning (Fig. 9). The E_{AR} was neither improved by the formation of homogeneous regions using catchment characteristics identified by a CCA analysis nor using catchment characteristics found to be related to hydrological characteristics via a sampling experiment (best-H).

4.3 Importance of catchment characteristics

The catchment characteristics which were important for the prediction of the ten SDH parameters in ungauged catchments are listed in Table 4. Catchment characteristics related to geology and hydrogeology were important for the prediction of the I_{BF}. Geology or more specifically the presence or non-presence of karstic rock was also important for the prediction of the SDH parameters related to the shape of the hydrograph (PDF location and PDF scale). On the contrary, catchment area was important for the prediction of the SDH parameters related to the magnitude of the event (GPD location, GPD scale, GEV location, and GEV scale). Exposition was meaningful for the prediction of the shape parameters of the marginal distributions of Q_p and V and the prediction of the dependence parameter θ.

5 Discussion

5.1 Comparison of regionalization methods

The results show that it is possible to regionalize the synthetic design hydrograph (SDH) parameters representing

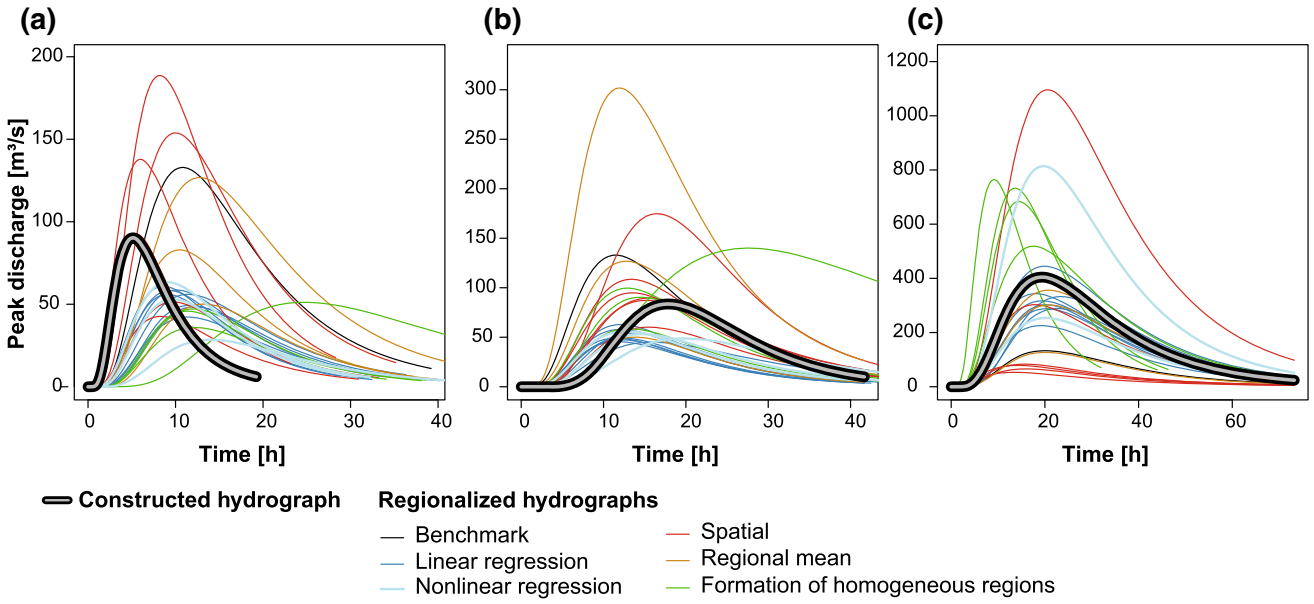

Fig. 7 Regionalized SDHs for three example catchments of different catchment size: Langete-Huttwil (60 km^2), Mentue-Yvonand (105 km^2), and Birs-Münchenstein (911 km^2) for different regionalization techniques: Benchmark model (black), Linear regression models (blue), nonlinear regression models (light blue), spatial methods (red), regional mean models (brown), formation of homogeneous regions (green). The hydrograph constructed based on observed runoff data is displayed in grey on black

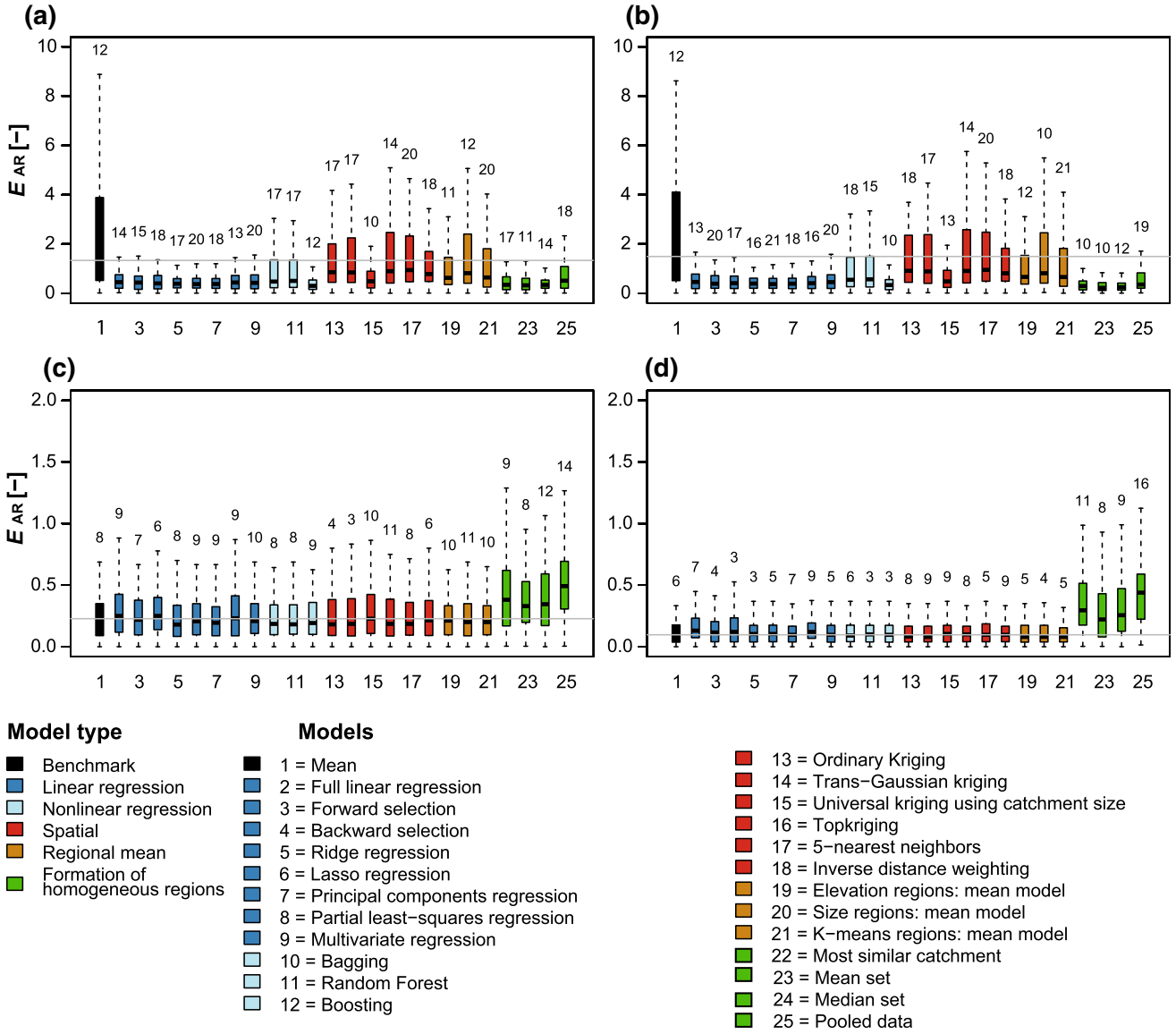

Fig. 8 Predictive performance of the different regionalization methods tested for the different hydrograph characteristics **a** peak discharge (Q_p), **b** hydrograph volume (V), **c** time to peak (t_p), and **d** half-recession time (t_{p05}) provided as boxplots of the absolute relative error (E_{AR}) for the 163 catchments. The number of outliers (defined as those observations lying outside the quartile ± 1.5 times the interquartile range) is indicated by the numbers plotted above the boxplots

the magnitude of the event in terms of peak discharge and hydrograph volume as well as the baseflow component. However, the results also indicate that the hydrograph shape represented by the two parameters of the PDF is difficult to regionalize. The two components of the hydrograph, magnitude and shape, are addressed in turn.

Hydrograph magnitude Nonlinear regression methods showed a good performance with respect to the SDH parameters related to the magnitude of the flood hydrograph and also performed better than other methods looking at the four hydrograph characteristics (Q_p, V, t_p, and t_{p05}). Boosting performed best among the nonlinear regression techniques. In contrast to bagging and random forest, boosting not only reduces variance by combining several trees but also reduces bias thanks to the stagewise procedure in which successive trees use information from previous trees. Regionalization using boosted regression trees resulted in a median relative error of 50% over the different catchments for the peak discharges and 55% for hydrograph volumes computed for a return period of 100 years. This is comparable to studies by Petroselli and Grimaldi (2015) and Viviroli et al. (2009a).

Some of the linear regression methods performed as well as the nonlinear methods for those SDH parameters that are linked to the marginal distributions of peak discharges and hydrograph volumes. However, linear

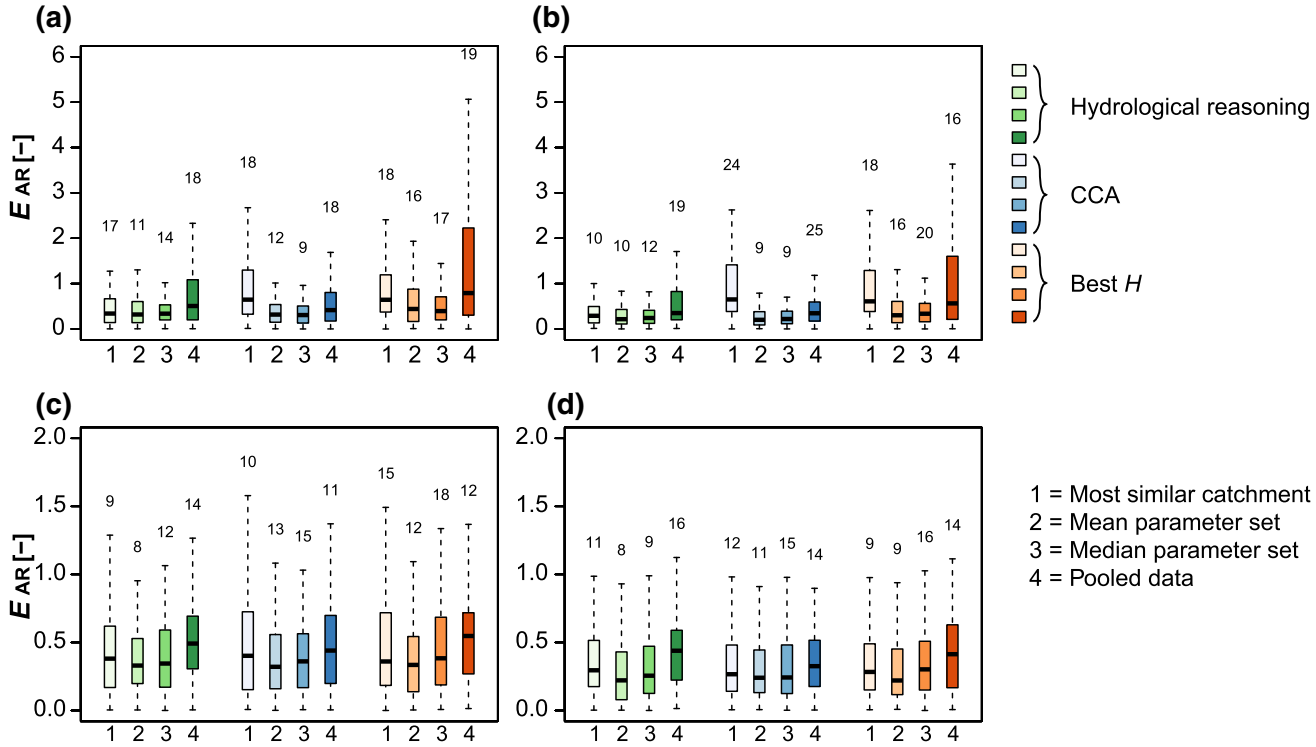

Fig. 9 Predictive performance of the regionalization methods based on the formation of homogeneous regions in terms of boxplots of the absolute relative error (E_{AR}) for the hydrograph characteristics **a** peak discharge, **b** hydrograph volume, **c** time to peak and **d** half-recession time of the hydrograph. The strategies used to form homogeneous regions are: hydrological reasoning (green), CCA (blue), and best-*H* (red). The methods used to transfer the parameter set to the target catchment from its five most similar catchments are: (1) Transfer from most similar catchment, (2) Transfer of mean parameter set from five most similar catchments, (3) Transfer of median parameter set from five most similar catchments, and (4) Estimation of the parameter set based on the pooled data from the five most similar catchments

Table 4 Catchment characteristics important for the prediction of the ten SDH parameters in ungauged catchments

Parameters related to hydrograph	SDH parameter	Important catchment characteristics
Magnitude	I_{BF}	Geology hard rock impermeable, X-coordinate, hydrogeology unconsolidated rock intermediate permeability
	GPD location	Catchment area, hydraulic topographic index standard deviation, length of main channel, relief energy
	GPD scale	Catchment area, maximum precipitation intensity over 24 h, hydraulic topographic index standard deviation
	GPD shape	West exposed surfaces, geology hard rock -pores, fissures, or karst, sunshine duration
	GEV location	Catchment area, hydraulic topographic index standard deviation, hydraulic conductivity skewness, relief energy
	GEV scale	Catchment area, hydraulic topographic index standard deviation, relief energy
	GEV shape	North exposed surfaces, maximum precipitation intensity, relief energy
	θ	South exposed surfaces, X-coordinate, hydrogeology hard rock impermeable, karstic rock, maximum precipitation during 24 h, average day of year
Shape	PDF location	Hydraulic topographic index skewness, forest, karstic rock
	PDF scale	Karstic rock, soil topographic index skewness, shape parameter 2

regression methods performed worse than nonlinear methods for the dependence between peak discharges and hydrograph volumes and the baseflow index. Yet, multiple regression methods have been found to be suitable for baseflow index regionalization by Haberlandt et al. (2001). Generally, some of the linear regression methods based on a reduction of the potential explanatory variables perform only slightly better than the full regression model. This might be related to the problem of finding appropriate explanatory variables.

Spatial methods could not compete with the regression methods when regionalizing the parameters of the marginal distributions of peak discharges and hydrograph volumes. The rather poor performance of kriging methods might be explained by the fact that the range of the empirical variogram was less than the mean distance between stations. However, they performed similarly well when regionalizing the dependence parameter and the baseflow index. The finding that regression-based methods generally perform better than spatial methods are in line with the recommendations made by the Centre for Eology and Hydrology (1999) but differ from observations made by Parajka et al. (2013), who analyzed 34 regionalization studies and concluded that regression-based methods are usually outperformed by spatial methods. He et al. (2011) found that spatial proximity was not helpful in all regionalization studies they reviewed because catchment characteristics can change abruptly in space. This is the case in Switzerland where even spatially close catchments can have quite different catchment characteristics. Spatial methods might perform better in regions with a high density of gauging stations (Merz 2006). In regions with fewer stations, such as in the alpine region, the uncertainty in the empirical variogram is expected to be larger (Blöschl 2006; Oudin et al. 2008). Among the spatial methods, universal kriging using catchment area as an explanatory variable clearly performed best when predicting the event magnitude. This is not surprising since we have seen that catchment area is one of the most important explanatory variables in the data set. Removing the scale effect of different catchment sizes is therefore very important. The other spatial methods did not differ significantly in their predictive performance. We did not find that top-kriging outperformed ordinary kriging as was found by Skoien et al. (2006). This is likely because spatial proximity does not necessarily entail similarity in hydrological behavior (Hrachowitz et al. 2013). In addition, the poor performance of top-kriging might also be related to the fact that not all the SDH parameters were well suited for the application of the top-kriging approach. The approach was developed for variables that accumulate along the stream network (Skoien et al. 2006), which is not necessarily the case for parameters of a statistical distribution.

The regional mean models led to a slight improvement compared to the global mean model (benchmark), which was also found by Sauquet and Catalogne (2011), but did not perform as well as regression methods for the regionalization of the flood magnitude. The methods transferring the entire parameter set from similar catchments to the target catchments led to good results in the prediction of peak discharges and hydrograph volumes. However, it was difficult to define regions that were homogeneous in terms of both catchment and hydrologic characteristics (*L*-moments of peak discharges) (Shu and Ouarda 2008) using all of the three strategies applied.

Hydrograph shape The two SDH parameters related to the hydrograph shape (PDF location and PDF scale) could not be satisfactorily regionalized. This means that no regionalization method could be found that outperformed the benchmark model. This finding was supported by the prediction error for the two hydrograph characteristics time to peak and half-recession time. This is in line with findings by Cipriani et al. (2012) who found that flood durations were more difficult to regionalize than flood quantiles. The reason for the poor performance in hydrograph shape regionalization might be that a part of the variability in flood shapes within a catchment was reduced when defining the representative normalized hydrograph (RNH) via the median hydrograph. As a consequence, RNHs across catchments were quite similar. Therefore, it is sufficient to work with one mean hydrograph shape across all catchments. Eventually, the nonparametric "distance-based" approach proposed by Ganora et al. (2009) for the regionalization of flow duration curves could be adjusted and successfully used for the regionalization of hydrograph shapes.

While the errors of the hydrograph volumes and peak discharges were correlated, errors in the hydrograph shape did not imply errors in the magnitude of the event. This means that even if an accurate prediction of the shape is not possible, the magnitude of the event can still be predicted accurately.

5.2 Best regionalization model

Hydrograph magnitudes were best regionalized using the nonlinear regression technique boosted regression trees while the mean model (benchmark) is the best model to regionalize the hydrograph shape. This difference shows that no universal regionalization method can be found (Razavi and Coulibaly 2013) for the regionalization of SDHs. One could take this into account by combining the two regionalization methods. Boosted regression trees could be applied to regionalize the SDH parameters related to the hydrograph magnitude while the mean model could be used for the regionalization of the SDH parameters

related to the hydrograph shape. Such a combined approach might lead to more accurate flood estimates in ungauged catchments than the use of one single method.

5.3 Important catchment characteristics for prediction

Different variables were important in fitting the different types of linear and nonlinear regression models for the ten SDH parameters. We again look first at the SDH parameters related to the hydrograph magnitude and then at the two SDH parameters related to the hydrograph shape.

Hydrograph magnitude

- Parameter baseflow: We found that geological and hydrogeological features were important for predicting the baseflow index, which is one of the most important low flow indices. Geological features have also been found to be important for the prediction of the baseflow index in other regions such as the Mediterranean (Longobardi and Villani 2008).
- Parameters marginal distributions: Similar catchment characteristics were important for the prediction of the location and scale parameters of the marginal distributions of peak discharges and hydrograph volumes. Namely, these were: catchment area, length of the main channel, maximum precipitation intensity, relief energy, and a parameter related to the topographic hydraulic index. Similar catchment characteristics were also found to be important in the prediction of flood quantiles by Ahn and Palmer (2016), Haddad and Rahman (2012) and Rahman et al. (2017). This is not surprising, because the magnitude of a flood is expected to increase with catchment size and the length of the main channel.
- Parameter dependence: Location in space and the exposition of surfaces was important for the prediction of the SDH parameter modeling the dependence between peak discharges and hydrograph volumes.

Hydrograph shape We found that the presence or absence of karstic rock is important for the prediction of the SDH parameters characterizing the hydrograph shape. However, no suitable regionalization method can be found for the SDH parameters related to the hydrograph shape, which means that it is a very weak explanatory variable.

5.4 Limitations

The regionalization of SDH parameters to ungauged catchments is hampered by three main factors: the lack of suitable catchment characteristics, the presence of uncertainties in both the computation of SDHs based on observed runoff and their regionalization, and by the fact that one hydrograph shape within a catchment is not representative of hydrograph shape variability.

Lack of suitable catchment characteristics The nonlinear regression methods take into account the fact that hydrological relationships are unlikely to be linear in nature (Aziz et al. 2015; Parajka et al. 2005) but they are unable to uncover underlying physical laws (He et al. 2011) like all regression based analyses. In addition, they cannot overcome the problem that the available catchment characteristics do not sufficiently explain the hydrological behavior and the flood generating processes of a catchment (Ali et al. 2012; Salinas et al. 2013). We need catchment characteristics that better represent the hydrological behavior of a catchment and an improved understanding of physical processes in a catchment to make a further step towards better prediction (He et al. 2011; Merz and Blöschl 2003; Oudin et al. 2010). However, the choice of relevant catchment characteristics is likely to be region and/or context dependent (Ali et al. 2012).

Uncertainties The quality of the regionalized values depends on two factors (Merz 2006): first, on the uncertainty of SDH estimates for gauged catchments; second, on the uncertainty inherent in the regionalization of those parameters. The uncertainty of the SDH parameters in the gauged catchments results from the length of the observation record, different model choices, and parameter estimation during the SDH construction process. The regionalization uncertainty can be considerable (Petroselli and Grimaldi 2015) and is among other sources of uncertainty related to the choice of a particular regionalization model out of a selection of coherent, sensible approaches. This source of uncertainty can be quantified thanks to this comprehensive comparison of regionalization methods. As an ensemble, the hydrographs obtained by the different regionalization methods give an idea of the variability introduced due to the choice of a regionalization model (McIntyre et al. 2005). For a more detailed analysis of both SDH construction and regionalization uncertainty, the reader is referred to the simulation study by Brunner et al. (2017a).

Misrepresentation of hydrograph shape variability Representing the hydrograph shape by just one catchment specific shape and regionalizing it with a mean model neglects the variability in flood shapes within a catchment. The hydrograph shape is only partly catchment specific and can differ significantly between different flood types, such as long-rain floods, short-rain floods, flash floods, or rain-on-snow floods (Sikorska et al. 2015).

5.5 Perspectives

The limitations mentioned above could be addressed as follows:

Identification of suitable catchment characteristics A better understanding of the influence of catchment characteristics on the flood response of a catchment might help to find suitable catchment characteristics for the regionalization of SDHs. However, the flood response is not only dependent on catchment characteristics but also on the particular weather pattern and antecedent wetness conditions that trigger the event. Nied et al. (2014) found that flood favoring hydro-meteorological patterns vary between seasons. They therefore claimed that flood frequency analysis should try to describe flood occurrence in dependence of hydro-meteorological patterns.

Uncertainty assessment To overcome the uncertainty related to the choice of the regionalization method, a combination of several methods as suggested by Merz (2006) might be appropriate. A combination of different methods, tested in this study, provides information on the variability of the design flood estimated for an ungauged catchment and could reduce the uncertainty related to a single estimate (Deutshe Vereinigung für Wasserwirtschaft Abwasser und Abfall 2012). Still, the uncertainty coming from the regionalization is not the only uncertainty source to be considered. The total uncertainty of an SDH in an ungauged catchment is also affected by the uncertainty of the data used for regionalization, i.e., the SDHs constructed based on observed runoff data.

Better representation of hydrograph shape variability The variability caused by different flood types could be accounted for by considering flood-type specific hydrograph shapes (Brunner et al. 2017b). These would take into account the heterogeneity of climatic inputs that make the prediction of a basin response difficult (Sivapalan 2003). However, we found that such flood-type specific hydrograph shapes are not very useful for regionalization since identifying groups of catchments with similar flood type patterns is difficult. We should therefore think about alternatives for the representation of the hydrograph shape variability within a catchment. Allowing for the representation of more than one shape type per catchment might reduce the uncertainty of the hydrograph shape estimates and therefore facilitate their regionalization.

6 Conclusions

We tested 24 methods, among them three nonlinear regression techniques not commonly applied in regionalization studies, for the regionalization of synthetic design hydrographs that provide information on the hydrograph peak and on the whole hydrograph including hydrograph volume, time to peak, and half-recession time. The extensive method comparison allowed for the identification of the most suitable regionalization method for synthetic design hydrographs. We showed that the regionalization of the design flood magnitude is possible, while the shape of the design flood remains difficult to regionalize. The parameters related to the hydrograph magnitude were best regionalized using the nonlinear approach of boosted regression trees. On the other hand, the mean model is sufficient to regionalize the parameters related to the hydrograph shape. Nonlinear regression methods were found to result in a better predictive performance than linear regression methods, spatial methods, and several other methods based on the formation of homogeneous regions. Spatial proximity alone was not able to explain the differences in design floods for different catchments. These differences can be better explained by different physiographical and climatological catchment characteristics. Among them, catchment area, length of the main channel, and relief energy were most important for the regionalization of SDH parameters related to the magnitude of the event. The relationship between these characteristics and the characteristics of the design flood are not always linear and are therefore best explained using nonlinear regression models. The regionalized design floods remain uncertain despite a comprehensive comparison of different regionalization methods. Uncertainties come from both the estimation of synthetic design hydrographs in gauged catchments and the regionalization of these hydrographs to ungauged catchments. These uncertainties need to be properly assessed in a simulation study to increase the reliability of the design hydrograph estimates. We recommend to use tree-based models such as bagging, random forest, and boosting in future regionalization studies. They can be especially useful when the relationship between a hydrological variable and different potential explanatory variables is complex.

Acknowledgements We thank the Federal Office for the Environment (FOEN) for funding the project (contract 13.0028.KP/M285-0623) and for providing runoff measurement data. We also thank MeteoSwiss for providing precipitation data. The data used in this study is available upon order from the FOEN and MeteoSwiss. For the hydrological data of the federal stations, the order form under http://www.bafu.admin.ch/wasser/13462/13494/15076/index.html?lang=de can be used. The hydrological data of the cantonal stations can be ordered from the respective cantons. The meteorological data can be ordered via https://shop.meteoswiss.ch/index.html. We thank the associate editor and the four reviewers for their constructive and detailed comments.

Appendix: List of stations used in this regionalization study

See Table 5.

Table 5 List of stations used in this regionalization study, a summary of their catchment characteristics, and their locally estimated SDH parameters (last ten columns)

ID	Station name	Area	ELEV	MELEV	DG	RL	Owner	I_{BF}	PDF location	PDF scale	GPD location	GPD scale	GPD shape	GEV location	GEV scale	GEV shape	θ
1	Aabach–Mönchaltorf	46	440	521	0	34	ZH	0.41	− 1.31	0.77	6	8.56	− 0.15	0.57	0.21	0.11	2.07
2	Aach–Salmsach	49	406	480	0	40	FOEN	0.39	− 1.08	0.61	4.7	6.39	− 0.15	0.49	0.17	0.17	1.97
3	Aire–Confignon	57	398	454	0	23	GE	0.3	− 1.1	0.44	6.9	15.89	− 0.25	0.75	0.22	0.15	1.91
4	Allenbach–Adelboden	29	1297	1856	0	40	FOEN	0.36	− 1.32	0.79	3.6	7.42	0.07	0.32	0.19	0.13	1.27
5	Alpbach–Erstfeld	21	1019	2200	28	41	FOEN	0.47	− 1.27	0.7	5.8	5.11	0.06	0.48	0.15	0.03	1.57
6	Alp–Einsiedeln	46	840	1155	0	23	FOEN	0.41	− 1.18	0.56	14.5	35.32	− 0.29	1.19	0.46	0.02	1.25
7	Altbach–Bassersdorf	13	470	549	0	37	ZH	0.42	− 0.77	0.42	1	1.41	− 0.04	0.1	0.04	0.13	1.97
8	Arbogne–Avenches	70	435	597	0	20	VD	0.58	− 0.97	0.5	3.1	3.83	− 0.09	0.24	0.1	0.3	2.24
9	Areuse–Boudry	377	444	1060	0	31	FOEN	0.35	− 0.88	0.64	47.6	17.59	− 0.07	6.07	1.72	0.08	3.41
10	Arnon–Grandson	83	434	942	0	20	VD	0.46	− 0.99	0.55	12.2	5.16	− 0.26	1.22	0.41	0.01	1.99
11	Aubonne–Allaman	91	390	890	0	35	FOEN	0.2	− 0.71	0.67	16.3	8.72	− 0.01	2.36	0.78	0.02	2.53
12	Augstbach–Balsthal	64	485	801	0	20	SO	0.36	− 1.04	0.59	5.4	6.35	0.19	0.58	0.23	0.19	1.71
13	Biber–Biberbrugg	32	825	1009	0	25	FOEN	0.33	− 0.82	0.55	7.7	16.51	− 0.55	0.74	0.3	0.13	1.56
14	Bibere–Kerzers	50	443	540	0	34	FOEN	0.61	− 0.95	0.66	2.5	2.98	0.07	0.16	0.07	0.24	2.13
15	Birse–Court	92	663	925	0	20	BE	0.53	− 1.06	0.64	7.1	8.45	− 0.18	0.55	0.22	0.01	1.65
16	Birse–Moutier	183	519	930	0	40	FOEN	0.58	− 0.91	0.49	12.9	11.05	− 0.13	0.94	0.35	0.14	1.92
17	Birse–Soyhières	590	395	810	0	28	FOEN	0.47	− 1	0.62	43.3	25.55	0.04	4.48	1.37	0.27	2.21
18	Birsig–Binningen	75	281	434	0	35	BL	0.5	− 1.11	0.66	3.6	4.26	0.05	0.34	0.14	0.2	1.77
19	Birs–Münchenstein	911	268	726	0	40	FOEN	0.47	− 1.02	0.56	66.8	31.15	0.02	6.84	1.98	0.2	2.65
20	Breggia–Chiasso	47	255	927	0	40	FOEN	0.23	− 1.08	0.51	12.9	27.95	− 0.11	1.69	0.61	0.03	1.81
21	Brinaz–Yverdon–les–Bains	14	434	542	0	20	VD	0.45	− 1.06	0.52	1.5	3.55	− 0.12	0.15	0.06	0.11	2.73
22	Broye–Payerne	392	441	710	0	40	FOEN	0.43	− 0.89	0.48	48.3	72.08	− 0.44	4.63	1.63	0.06	1.82
23	Bruggbach–Gipf/Oberfrick	45	356	575	0	35	AG	0.38	− 1.09	0.64	3.6	6.51	− 0.16	0.4	0.16	0.13	1.53
24	Bünz–Muri (Hasli)	15	448	613	0	30	AG	0.9	− 0.74	0.44	1.3	2.33	0.14	0.1	0.04	0.2	1.76
25	Bünz–Othmarsingen	111	390	533	0	37	AG	0.56	− 0.61	0.4	6.8	6.87	0.02	0.49	0.19	0.36	2.12
26	Bünz–Wohlen	53	421	555	0	34	AG	0.53	− 0.92	0.46	3.3	5.45	− 0.07	0.26	0.12	0.4	2.23
27	Buuserbach–Maisprach	11	367	529	0	36	BL	0.65	− 1.03	0.62	0.6	0.64	0.01	0.04	0.02	0.15	1.35
28	Cassarate–Pregassona	74	291	990	0	40	FOEN	0.4	− 0.76	0.62	9.5	15.69	0	1.21	0.53	0.13	1.65
29	Chämtnerbach– Wetzikon	13	560	760	0	29	ZH	0.4	− 0.61	0.29	1.9	3.62	− 0.06	0.17	0.07	0.18	1.81
30	Chandon–Avenches	39	432	571	0	20	VD	0.66	− 0.68	0.36	1.8	3.64	0.07	0.09	0.04	0.54	2.34
31	Chli Schliere–Alpnach	22	453	1370	0	36	FOEN	0.38	− 0.8	0.55	4.4	8.83	0.04	0.37	0.14	0.32	1.94
32	Chrebsbach–St. Margarethen	14	503	581	0	21	TG	0.39	− 1.3	0.74	1.2	3.88	− 0.21	0.12	0.05	0.21	1.92
33	Diegterbach–Diegten	13	509	746	0	31	BL	0.43	− 1.16	0.67	1.4	2.28	0.06	0.11	0.05	0.23	1.35

Table 5 (continued)

ID	Station name	Area	ELEV	MELEV	DG	RL	Owner	I_{BF}	PDF location	PDF scale	GPD location	GPD scale	GPD shape	GEV location	GEV scale	GEV shape	θ
34	Diegterbach–Sissach	33	372	614	0	36	BL	0.32	− 1.15	0.58	2.7	5.11	− 0.13	0.29	0.11	0.29	1.58
35	Dorfbach–Allschwil	11	281	360	0	30	BL	0.59	− 1.16	0.67	0.3	0.48	0.43	0.02	0.01	0.43	2.75
36	Drize–Lancy	23	392	528	0	25	GE	0.32	− 1.33	0.65	2	4.33	− 0.23	0.22	0.08	0.17	2.09
37	Dünnern–Olten	196	400	750	0	36	FOEN	0.37	− 1.15	0.53	16.6	20.52	− 0.11	1.8	0.7	0.16	1.9
38	Eibach–Gelterkinden	27	405	627	0	36	BL	0.23	− 0.99	0.67	2.4	2.78	0.12	0.3	0.11	0.17	1.66
39	Eibach–Zeglingen	13	517	725	0	30	BL	0.35	− 1.1	0.68	1.2	1.51	0.21	0.13	0.05	0.13	1.55
40	Emme–Eggiwil	124	745	1189	0	39	FOEN	0.29	− 0.96	0.49	27.1	44.22	− 0.21	2.68	0.99	0.08	1.53
41	Emme–Wiler	939	458	860	0	40	FOEN	0.54	− 0.64	0.38	84.2	80.96	− 0.01	6.01	2.06	0.21	1.66
42	Ergolz–Itingen	141	350	593	0	33	BL	0.34	− 1.02	0.6	10	10.26	0	1.14	0.39	0.23	1.76
43	Ergolz–Liestal	261	305	590	0	40	FOEN	0.34	− 1	0.66	19.9	20.27	0	2.25	0.78	0.23	2.16
44	Ergolz–Ormalingen	30	410	585	0	36	BL	0.24	− 1	0.66	2.4	3.55	− 0.01	0.33	0.13	0.21	1.93
45	Etzgerbach–Etzgen	25	308	478	0	34	AG	0.45	− 0.9	0.45	2.4	4.07	− 0.1	0.19	0.06	0.19	1.46
46	Eulach–Wülflingen	73	410	532	0	43	ZH	0.35	− 1.22	0.57	4.1	9.54	− 0.05	0.42	0.2	0.21	1.46
47	Fisibach–Fisibach	15	379	516	0	31	AG	0.65	− 0.63	0.56	0.6	0.72	0.09	0.03	0.01	0.3	1.85
48	Flon–Oron–la− Ville	16	609	812	0	20	VD	0.25	− 1.19	0.76	2.2	3.88	− 0.18	0.25	0.09	0.17	2.14
49	Furtbach–Würenlos	39	410	482	0	36	ZH	0.57	− 1.08	0.63	2.8	2.11	− 0.05	0.22	0.08	0.13	1.99
50	Geisslibach–Furtmüli	20	415	474	0	24	ZH	0.68	− 0.48	0.31	0.6	0.63	0.01	0.04	0.02	0.24	1.59
51	Glatt–Herisau	16	679	840	0	40	FOEN	0.45	− 0.93	0.51	3.3	5.84	0.33	0.26	0.11	0.04	1.72
52	Goldach–Goldach	50	399	833	0	23	FOEN	0.42	− 1.28	0.82	8.2	13.82	0.05	0.76	0.33	0.2	1.71
53	Goneri–Oberwald	40	1385	2377	14	23	FOEN	0.55	− 0.85	0.43	7.2	9.82	− 0.02	0.64	0.24	0.21	1.85
54	Grenet (amont)–Pigeon	19	680	748	0	20	VD	0.27	− 1.26	0.54	4.4	8.53	− 0.42	0.45	0.14	0.02	1.23
55	Grossbach–Gross	11	900	1235	0	40	FOEN	0.36	− 0.57	0.36	2.5	4.23	0.07	0.2	0.08	0.07	1.28
56	Grosstalbach–Isenthal	44	767	1820	9	40	FOEN	0.59	− 1.19	0.8	5	3.26	0.33	0.39	0.15	0.13	1.73
57	Gürbe–Belp	117	511	837	0	40	FOEN	0.55	− 1.01	0.55	14.9	9.54	− 0.21	0.85	0.27	0.07	1.36
58	Gürbe–Burgistein	54	568	1044	0	28	FOEN	0.43	− 1.2	0.69	7	8.87	− 0.01	0.61	0.2	0.17	1.44
59	Haselbach–Maschwanden	20	390	495	0	37	ZH	0.51	− 0.8	0.63	1.7	2.72	− 0.17	0.14	0.06	0.26	2.34
60	Hintere Frenke–Bubendorf	38	352	603	0	30	BL	0.33	− 1.08	0.68	3.1	3.44	0.05	0.37	0.13	0.14	1.73
61	Hintere Frenke–Reigoldswil	15	489	742	0	32	BL	0.47	− 1.1	0.72	1.6	1.2	0.2	0.15	0.05	0.18	1.79
62	Hinterrhein–Hinterrhein	54	1584	2360	17	35	FOEN	0.58	− 0.71	0.58	16.5	20.93	− 0.04	1.09	0.42	0.22	1.82
63	Holzbach–Villmergen	24	416	590	0	34	AG	0.52	− 1.04	0.7	1.4	1.93	− 0.06	0.11	0.05	0.34	1.85
64	Homburgerbach–Thürnen	30	387	615	0	36	BL	0.2	− 0.94	0.6	2.2	2.3	0.09	0.29	0.09	0.14	1.59
65	Ilfis–Langnau	188	685	1051	0	25	FOEN	0.48	− 0.87	0.38	25.6	44.32	− 0.01	2.16	0.78	0.27	1.8
66	Jona–Pilgersteg	24	560	818	0	44	ZH	0.46	− 1.01	0.56	5.4	7.01	− 0.09	0.47	0.17	0.1	1.69
67	Jona–Rüti	58	450	669	0	20	ZH	0.43	− 0.72	0.44	11.1	13.67	− 0.15	0.96	0.39	0.17	2.03

Table 5 (continued)

ID	Station name	Area	ELEV	MELEV	DG	RL	Owner	I_{BF}	PDF location	PDF scale	GPD location	GPD scale	GPD shape	GEV location	GEV scale	GEV shape	θ
68	Jonen–Zwillikon	39	460	605	0	27	ZH	0.42	− 0.98	0.56	3.3	4.64	0.07	0.32	0.13	0.26	2.06
69	Kaisterbach–Kaisten	12	321	464	0	34	AG	0.51	− 0.95	0.5	0.8	1.59	0.08	0.06	0.02	0.23	1.51
70	Kander–Hondrich	520	650	1900	8	33	FOEN	0.72	− 0.82	0.51	47.9	23.93	− 0.06	2.67	0.94	0.08	1.94
71	Kempt–Fehraltorf	24	520	645	0	23	ZH	0.47	− 1.04	0.49	1.9	2.98	0.07	0.17	0.08	0.25	2.4
72	Kempt–Winterthur	60	450	588	0	33	ZH	0.5	− 1.1	0.51	6.3	5.75	0.05	0.56	0.22	0.18	2.14
73	Kleine Emme–Littau	477	431	1050	0	36	FOEN	0.45	− 0.67	0.41	84.5	119.79	− 0.18	6.63	2.25	0.17	1.75
74	Kleine Emmev–Werthenstein	311	540	1173	0	30	FOEN	0.45	− 0.97	0.62	56.7	74.78	− 0.14	4.55	1.61	0.16	1.77
75	Köllikerbach–Kölliken	10	423	488	0	31	AG	0.47	− 0.79	0.43	1.2	2.99	− 0.19	0.08	0.04	0.17	1.38
76	Langeten–Huttwil	60	597	766	0	40	FOEN	0.6	− 1	0.57	4	5.51	0.11	0.24	0.1	0.23	1.58
77	Langeten–Lotzwil	115	500	713	0	20	BE	0.66	− 1.05	0.75	5.8	1.46	− 0.11	0.31	0.11	− 0.1	1.35
78	Lonza–Blatten	78	1520	2630	37	40	FOEN	0.43	− 1	0.92	11.6	8.83	− 0.15	1.17	0.45	− 0.08	1.11
79	Louibach–Saanen	62	1085	1875	6	20	BE	0.64	− 0.82	0.51	8.4	4.98	− 0.22	0.48	0.18	0.09	1.45
80	Luthern–Nebikon	108	494	740	0	26	FOEN	0.49	− 0.89	0.51	6.5	9.9	− 0.07	0.58	0.21	0.24	1.93
81	Lyssbach–Lyss	50	444	574	0	22	BE	0.65	− 0.6	0.31	3.1	6.45	− 0.26	0.16	0.06	0.33	1.98
82	Lyssbach–Schüpfen	23	505	616	0	22	BE	0.65	− 0.31	0.31	1.1	2.32	− 0.11	0.06	0.02	0.43	1.94
83	Magdenerbach–Rheinfelden	33	300	483	0	31	AG	0.46	− 1.05	0.96	1.8	2.64	− 0.11	0.18	0.07	0.17	1.98
84	Magliasina–Magliaso	34	295	920	0	34	FOEN	0.3	− 0.95	0.56	6	7.92	0.18	0.77	0.33	0.2	1.99
85	Marchbach–Oberwil	27	296	462	0	34	BL	0.58	− 1.1	0.99	1.2	2.12	− 0.01	0.08	0.04	0.33	1.57
86	Mederbach–Marthalen	26	375	439	0	46	ZH	0.52	− 0.99	0.63	0.6	0.84	0.03	0.06	0.03	0.24	1.62
87	Mederbach–Niederwiesen	30	368	425	0	30	ZH	0.55	− 1.01	0.66	0.6	0.6	− 0.22	0.05	0.03	0.12	1.17
88	Mentue–Yvonand	105	449	679	0	40	FOEN	0.48	− 0.68	0.41	9.3	14.69	− 0.25	0.81	0.29	0.17	1.71
89	Minster–Euthal	59	894	1351	0	40	FOEN	0.36	− 0.41	0.34	18.5	43.01	− 0.22	1.58	0.61	0.09	1.21
90	Möhlinbach–Zeiningen	27	338	514	0	32	AG	0.41	− 1.19	0.81	1.6	1.92	− 0.1	0.16	0.06	0.11	1.83
91	Murg–Frauenfeld	212	390	580	0	40	FOEN	0.49	− 1	0.62	18.4	22.27	− 0.04	1.77	0.69	0.12	2.41
92	Murg–Murgenthal	207	419	637	0	34	FOEN	0.65	− 1.02	0.73	11.2	7.68	− 0.1	0.61	0.22	0.13	1.51
93	Murg–Wängi	79	466	650	0	40	FOEN	0.44	− 0.85	0.41	8.6	8.52	− 0.11	0.83	0.3	0.02	2.1
94	Näfbach–Neftenbach	38	394	464	0	22	ZH	0.56	− 0.85	0.44	2	2.44	0.08	0.16	0.07	0.23	1.97
95	Necker–Mogelsberg	88	606	959	0	40	FOEN	0.35	− 0.62	0.4	20.3	26.47	0.14	1.95	0.72	0.18	1.82
96	Nozon–Pré Chaillet	45	440	882	0	21	VD	0.28	− 0.96	0.61	3.1	1.48	− 0.04	0.37	0.09	0.24	2.6
97	Önz–Heimenhusen	84	440	583	0	20	BE	0.73	− 0.84	0.51	4	3.02	− 0.21	0.17	0.06	0.33	1.7
98	Orbe–Le Sentier	96	1010	1210	0	21	VD	0.34	− 0.9	0.56	9.8	3.6	− 0.07	1.16	0.31	0	2.37
99	Orisbach–Liestal	21	315	515	0	33	BL	0.2	− 0.91	0.76	1.4	2.07	0.09	0.21	0.08	0.4	2.09
100	Ova dal Fuorn–Zernez	55	1707	2331	0	40	FOEN	0.5	− 1.16	0.62	1.7	1.91	− 0.1	0.13	0.07	0.26	2.04

Table 5 (continued)

ID	Station name	Area	ELEV	MELEV	DG	RL	Owner	I_{BF}	PDF location	PDF scale	GPD location	GPD scale	GPD shape	GEV location	GEV scale	GEV shape	θ
101	Petite Glâne–Villars-le-Grand	85	433	560	0	20	VD	0.52	− 0.92	0.56	4.8	7.72	− 0.36	0.44	0.18	0.17	2.24
102	Pfaffnern–Vordemwald	39	417	517	0	34	AG	0.55	− 0.47	0.32	3.2	7.22	− 0.11	0.22	0.1	0.3	1.74
103	Plessur–Chur	263	573	1850	0	40	FOEN	0.57	− 0.92	0.72	12	12	− 0.07	1.26	0.56	0.1	2.47
104	Poschiavino–La Rösa	14	1860	2283	0	40	FOEN	0.53	− 1.12	0.56	1.4	1.94	− 0.02	0.13	0.06	0.32	2.24
105	Promenthouse–Gland	100	394	1037	0	28	FOEN	0.26	− 0.68	0.79	4.8	4.62	0.24	0.65	0.22	0.32	2.79
106	Reppisch–Birmensdorf	24	466	665	0	44	ZH	0.31	− 1.15	0.73	1.6	2.24	0.18	0.2	0.08	0.32	1.85
107	Reppisch–Dietikon	69	380	594	0	28	ZH	0.45	− 1.09	0.6	5.4	8.81	0.09	0.55	0.25	0.27	2.45
108	Riale di Pincascia–Lavertezzo	44	536	1708	0	22	FOEN	0.34	− 0.93	0.41	25.5	28.99	0.03	2.68	0.96	− 0.02	1.52
109	Rot–Roggwil	54	436	586	0	25	FOEN	0.57	− 0.64	0.41	4	5.88	− 0.1	0.25	0.09	0.23	1.58
110	Ruederchen–Schöftland	19	463	614	0	34	AG	0.51	− 0.78	0.47	1.2	2.59	0.03	0.09	0.04	0.27	1.8
111	Scheulte–Vicques	73	463	785	0	22	FOEN	0.46	− 1.01	0.48	8	10.34	0.07	0.8	0.31	0.27	2.63
112	Schmittenbach–Remigen	13	385	523	0	32	AG	0.09	− 0.88	0.71	0.9	0.98	0.12	0.15	0.06	0.23	2.99
113	Schwarzenbach–Rickenbach	15	410	454	0	22	ZH	0.52	− 0.72	0.4	1	1.52	− 0.16	0.08	0.03	0.39	2.04
114	Sellenbodenbach–Neuenkirch	11	515	615	0	23	FOEN	0.32	− 1.14	0.53	1.5	5.16	0	0.14	0.06	0.36	1.84
115	Sense–Thörishaus	352	555	1068	0	36	FOEN	0.48	− 1.03	0.58	46	58.77	− 0.12	3.4	1.11	0.14	1.25
116	Seymaz–Thônex	37	393	451	0	20	GE	0.43	− 0.99	0.53	3	2.92	− 0.08	0.31	0.11	0.18	2.41
117	Seyon–Valangin	112	630	970	0	34	FOEN	0.36	− 1.01	0.49	5.8	8.85	− 0.31	0.62	0.22	0.22	2.22
118	Simme–Oberried/Lenk	36	1096	2370	35	40	FOEN	0.34	− 0.99	0.71	5.2	4.62	− 0.12	0.59	0.28	− 0.08	1.71
119	Simme–Oberwil	344	777	1640	4	40	FOEN	0.58	− 1.15	0.55	30.7	18.24	− 0.02	2.33	0.83	0.11	2
120	Simme–Zweisimmen	203	930	1801	6	21	BE	0.61	− 1.06	0.65	20.2	12.99	− 0.07	1.46	0.58	0.21	2.03
121	Sinserbach–Sins	16	415	561	0	33	AG	0.33	− 1.45	0.71	1.3	3.01	0.12	0.14	0.06	0.22	2.01
122	Sionge–Vuippens	45	681	862	0	39	FOEN	0.4	− 1.11	0.62	7	10.98	− 0.24	0.68	0.23	0.09	1.58
123	Sissle–Eiken	123	314	529	0	37	AG	0.19	− 0.98	0.62	9.2	11.68	− 0.05	1.16	0.43	0.17	1.85
124	Sissle–Hornussen	37	365	524	0	35	AG	0.26	− 1.06	0.62	3	4.82	− 0.1	0.38	0.14	0.2	1.59
125	Somvixer Rhein–Somvix	22	1490	2450	7	36	FOEN	0.53	− 0.69	0.46	6.8	5.94	0.18	0.49	0.2	0.02	1.5
126	Sorne–Delémont	241	406	808	0	31	FOEN	0.44	− 0.96	0.7	17.1	7.75	0.03	1.83	0.51	0.17	2.38
127	Staffeleggbach–Frick	21	358	534	0	35	AG	0.3	− 1.01	0.69	1.5	1.96	− 0.02	0.18	0.07	0.15	1.69
128	Steinach–Steinach	24	406	710	0	30	FOEN	0.53	− 1.06	0.85	4.4	8.3	− 0.09	0.28	0.1	0.25	1.46
129	Steinenbach–Kaltbrunn	19	451	1112	0	30	FOEN	0.37	− 0.74	0.45	6.4	15.9	− 0.54	0.56	0.19	0.09	1.54
130	Stichbach–Bottighofen	16	410	522	0	22	TG	0.31	− 1.39	0.6	1.1	2.03	0.3	0.13	0.06	0.41	3.06
131	Surb–Döttingen	67	335	511	0	34	AG	0.58	− 0.74	0.42	3.8	4.88	0.05	0.26	0.11	0.28	2.01
132	Surb–Unterehrendingen	28	424	541	0	21	AG	0.59	− 0.3	0.37	2.2	3.38	0.07	0.15	0.06	0.28	2.2

Table 5 (continued)

ID	Station name	Area	ELEV	MELEV	DG	RL	Owner	I_{BF}	PDF location	PDF scale	GPD location	GPD scale	GPD shape	GEV location	GEV scale	GEV shape	θ
133	Suze–Sonceboz	150	642	1050	0	53	FOEN	0.43	− 0.95	0.59	15.4	4.97	0.14	1.53	0.47	0.11	2.87
134	Tägerbach-Wislikofen	14	390	551	0	32	AG	0.71	− 0.9	0.79	0.4	0.46	− 0.21	0.02	0.01	0.2	1.41
135	Talbach–Schinznach-Dorf	15	360	552	0	34	AG	0.19	− 0.97	0.76	0.6	1.4	0.22	0.07	0.03	0.05	1.5
136	Talent–Chavornay	66	440	670	0	20	VD	0.43	− 1.05	0.54	8	10.81	− 0.28	0.76	0.26	0.12	1.67
137	Taschinasbach-Grüsch	63	666	1768	0	34	FOEN	0.39	− 1.23	0.67	9.2	9.63	0.07	0.92	0.39	0.09	2.05
138	Thur–Andelfingen	1696	356	770	0	40	FOEN	0.49	− 0.85	0.44	230.9	142.25	− 0.1	19.05	5.77	0.25	2.21
139	Thur–Halden	1085	456	910	0	40	FOEN	0.49	− 1.16	0.58	205.2	178.62	− 0.13	16.28	5.52	0.17	1.93
140	Thur–Jonschwil	493	534	1030	0	40	FOEN	0.42	− 0.87	0.42	113.1	116.86	− 0.2	10.36	3.17	0.18	1.96
141	Thur–Stein	84	850	1448	0	31	FOEN	0.36	− 0.92	0.46	17.2	14.14	0.02	1.93	0.62	0.23	2.6
142	Töss–Altlandenberg	67	621	871	0	36	ZH	0.24	− 1.03	0.61	12.6	14.8	0.01	1.51	0.53	0.16	2.19
143	Töss–Freienstein	399	360	626	0	29	ZH	0.51	− 1.13	0.6	36.4	26.99	0.14	3.54	1.19	0.17	2.72
144	Töss–Neftenbach	342	389	650	0	40	FOEN	0.48	− 0.98	0.52	34.8	30.17	0.04	3.53	1.19	0.17	2.65
145	Töss–Rämismühle	127	524	790	0	35	ZH	0.31	− 1.04	0.56	20.4	19.06	− 0.05	2.37	0.73	0.18	2.07
146	Trübbach–Räzliberg	20	1430	2610	54	22	FOEN	0.2	− 1.38	0.68	2.9	2.89	− 0.19	0.28	0.14	0.05	1.13
147	Ürke–Holziken	25	438	577	0	35	AG	0.66	− 0.86	0.53	1.3	1.97	− 0.23	0.07	0.03	0.27	1.36
148	Urnäsch–Hundwil	65	746	1085	0	33	FOEN	0.4	− 1.02	0.51	16.8	20.69	− 0.05	1.46	0.51	0.09	1.49
149	Vedeggio–Bioggio	95	280	950	0	35	FOEN	0.33	− 0.89	0.64	15.2	24.87	0.11	2	0.79	0.25	1.67
150	Venoge–Ecublens	231	383	700	0	35	FOEN	0.4	− 0.9	0.62	16	14.37	− 0.07	2.15	0.69	0.28	3.51
151	Verzasca–Lavertezzo	186	490	1672	0	24	FOEN	0.45	− 0.84	0.4	74.3	124.12	− 0.08	7.55	2.7	− 0.12	1.8
152	Veveyse–Vevey	62	425	1108	0	30	FOEN	0.39	− 1.08	0.64	12.4	21.31	− 0.13	1.01	0.37	0	1.27
153	Violenbach–Augst	17	268	425	0	35	BL	0.29	− 1.08	0.73	0.9	1.39	− 0.02	0.1	0.04	0.14	1.41
154	Vordere Frenke–Bubendorf	46	371	647	0	36	BL	0.46	− 1.02	0.5	3.6	4.44	− 0.12	0.33	0.12	0.18	1.67
155	Vordere Frenke–Waldenburg	13	524	826	0	35	BL	0.24	− 0.82	0.58	1.1	1.53	− 0.17	0.12	0.05	0.25	1.42
156	Weisse Lütschine–Zweilütschinen	164	650	2170	18	40	FOEN	0.56	− 1.09	0.77	21.6	15.31	− 0.15	1.75	0.65	− 0.09	1.48
157	Werrikerbach–Greifensee	12	440	493	0	21	ZH	0.49	− 0.99	1.17	0.4	0.18	− 0.01	0.03	0.01	− 0.1	1.42
158	Wigger–Zofingen	368	426	660	0	35	FOEN	0.56	− 0.85	0.53	21.4	23.91	− 0.11	1.52	0.6	0.23	1.68
159	Wissenbach–Boswil	12	460	684	0	34	AG	0.39	− 1.17	0.61	0.7	1	0.2	0.07	0.03	0.2	1.61
160	Wölflinswiler Bach–Wittnau	17	395	600	0	30	AG	0.39	− 1	0.59	1.5	3.03	− 0.19	0.16	0.06	0.15	1.69
161	Wyna–Reinach	47	514	682	0	30	AG	0.53	− 0.39	0.32	4	4.86	− 0.02	0.31	0.12	0.22	1.86
162	Wyna–Suhr	120	392	617	0	34	AG	0.5	− 0.91	0.61	6.9	9.68	− 0.21	0.6	0.24	0.28	1.82

Table 5 (continued)

ID	Station name	Area	ELEV	MELEV	DG	RL	Owner	I_{BF}	PDF location	PDF scale	GPD location	GPD scale	GPD shape	GEV location	GEV scale	GEV shape	θ
163	Wyna–Unterkulm	92	455	649	0	37	AG	0.53	− 0.79	0.48	7	9.29	− 0.18	0.56	0.21	0.26	1.62

The station name is provided together with a catchment ID, catchment area [km^2], elevation [m.a.s.l.] (ELEV), mean elevation [m.a.s.l.] (MELEV), degree of glaciation [%] (DG), record length [a] (RL), and the owner of the station. Data owners are the Federal Office for the Environment (FOEN), and different cantons: Zürich (ZH), Vaud (VD), Solothurn (SO), Bern (BE), Baselland (BL), Aargau (AG), and Thurgau (TG). The SDH parameters are explained in Fig. 2

References

Abrahart RJ, See LM (2007) Neural network modelling of non-linear hydrological relationships. Hydrol Earth Syst Sci 11:1563–1579. https://doi.org/10.5194/hess-11-1563-2007

Acreman MC, Sinclair CD (1986) Classification of drainage basins acording to their physical characteristics; an application for flood frequency analysis in Scotland. J Hydrol 84:365–380. https://doi.org/10.1016/0022-1694(86)90134-4

Ahn KH, Palmer R (2016) Regional flood frequency analysis using spatial proximity and basin characteristics: quantile regression versus parameter regression technique. J Hydrol 540:515–526. https://doi.org/10.1016/j.jhydrol.2016.06.047

Ali G, Tetzlaff D, Soulsby C, McDonnell JJ, Capell R (2012) A comparison of similarity indices for catchment classification using a cross-regional dataset. Adv Water Resour 40:11–22. https://doi.org/10.1016/j.advwatres.2012.01.008

Archfield SA, Pugliese A, Castellarin A, Skøien JO, Kiang JE (2013) Topological and canonical kriging for design flood prediction in ungauged catchments: an improvement over a traditional regional regression approach? Hydrol Earth Syst Sci 17(4):1575–1588. https://doi.org/10.5194/hess-17-1575-2013

Aziz K, Rai S, Rahmen A (2015) Design flood estimation in ungauged catchments using genetic algorithm-based artificial neural network (GAANN) technique for Australia. Nat Hazards 77:805–821. https://doi.org/10.1007/s11069-015-1625-x

Aziz K, Haque MM, Rahman A, Shamseldin AY, Shoaib M (2016) Flood estimation in ungauged catchments: application of artificial intelligence based methods for Eastern Australia. Stoch Env Res Risk Assess. https://doi.org/10.1007/s00477-016-1272-0

Bardossy A (2007) Calibration of hydrological model parameters for ungauged catchments. Hydrol Earth Syst Sci 11:703–710

Bardossy A, Lehmann W (1997) Spatial distribution of soil moisture in a small catchment. Part 1: geostatistical analysis. J Hydrol 206:1–15. https://doi.org/10.1016/S0022-1694(97)00152-2

Beygelzimer A, Kakadet S, Langford J, Arya S, Mount D, Li S (2013) Package 'FNN': fast nearest neighbor search algorithms and applications. http://cran.r-project.org/package=FNN

Bhunya PK, Panda SN, Goel MK (2011) Synthetic unit hydrograph methods: a critical review. Open Hydrol J 5:1–8. https://doi.org/10.2174/1874378101105010001

Bitterli T, Aviolat P, Brändli R, Christe R, Fracheboud S, Frey D, George M, Matousek F, Tripet JP (2007) Groundwater resources. In: Hydrological Atlas of Switzerland, Bern, p 8.6

Blöschl G (2006) Geostatistische Methoden bei der hydrologischen Regionalisierung. In: Godina R, Blöschl G (eds) Methoden der hydrologischen Regionalisierung, vol 197. Wiener Mitteilungen, Wien, pp 21–40

Blöschl G, Sivapalan M, Wagener T, Viglione A, Savenije H (2013) Runoff prediction in ungauged basins. Cambridge University Press, Cambridge

Boscarello L, Ravazzani G, Cislaghi A, Mancini M (2016) Regionalization of flow-duration curves through catchment classification with streamflow signatures and physiographic-climate indices. J Hydrol Eng. https://doi.org/10.1061/(ASCE)HE.1943-5584.0001307

Breiman L (1996) Bagging predictors. Mach Learn 24(421):123–140. https://doi.org/10.1007/BF00058655

Breiman L (2001) Random Forests. Mach Learn 45(1):5–32. https://doi.org/10.1023/A:1010933404324

Brunner MI, Seibert J, Favre AC (2016) Bivariate return periods and their importance for flood peak and volume estimation. Wire's Water 3:819–833. https://doi.org/10.1002/wat2.1173

Brunner MI, Sikorska AE, Furrer R, Favre AC (2017a) Uncertainty assessment of synthetic design hydrographs for gauged and ungauged catchments. Water Resour Res **(accepted)**

Brunner MI, Viviroli D, Sikorska AE, Vannier O, Favre AC, Seibert J (2017b) Flood type specific construction of synthetic design hydrographs. Water Resour Res. https://doi.org/10.1002/2016WR019535

Bundesamt für Statistik (2003) Geodaten der Bundesstatistik. https://www.bfs.admin.ch/bfs/de/home/dienstleistungen/geostat/geodaten-bundesstatistik.html

Burn DH (1989) Cluster analysis as applied to regional flood frequency. J Water Resour Plan Manag 115:567–582

Burn DH (1990) Evaluation of regional flood frequency analysis with a region of influence approach. Water Resour Res 26(10):2257–2265. https://doi.org/10.1029/WR026i010p02257

Burn DH, Boorman DB (1992) Catchment classification applied to the estimation of hydrological parameters at ungauged catchments. Tech. rep, Institute of Hydrology, Wallingford, Oxfordshire

Burn DH, Boorman DB (1993) Estimation of hydrological parameters at ungauged catchments. J Hydrol 143:429–454. https://doi.org/10.1016/0022-1694(93)90203-L

Camezind-Wildi R (2005) Empfehlung Raumplanung und Naturgefahren. Tech. rep., Bundesamt für Raumentwicklung, Bundesamt für Wasser und Geologie, Bundesamt für Umwelt, Wald und Landschaft, Bern

Castellarin A, Burn DH, Brath A (2001) Assessing the effectiveness of hydrological similarity measures for flood frequency analysis. J Hydrol 241(3):270–285. https://doi.org/10.1016/S0022-1694(00)00383-8

Castiglioni S, Castellarin A, Montanari A, Skøien JO, Laaha G, Blöschl G (2011) Smooth regional estimation of low-flow indices: physiographical space based interpolation and top-kriging. Hydrol Earth Syst Sci 15(3):715–727. https://doi.org/10.5194/hess-15-715-2011

Cavadias GS, Ouarda TBMJ, Bobée B, Girard C (2001) A canonical correlation approach to the determination of homogeneous regions for regional flood estimation of ungauged basins. Hydrol Sci J 46(4):499–512. https://doi.org/10.1080/02626660109492846

Centre for Ecology and Hydrology (1999) Flood estimation handbook. Centre for Ecology and Hydrology, Wallingford, Oxfordshire

Chapman TG, Maxwell AI (1996) Baseflow separation–comparison of numerical methods with tracer experiments. 23rd hydrology and water resources symposium. Hobart, Australia, pp 539–545

Chebana F, Ouarda T (2009) Multivariate quantiles in hydrological frequency analysis. Environmetrics 22:63–78. https://doi.org/10.1002/env.1027

Cheng L, Yaeger M, Viglione A, Coopersmith E, Ye S, Sivapalan M (2012) Exploring the physical controls of regional patterns of flow duration curves—Part 1: insights from statistical analyses. Hydrol Earth Syst Sci 16:4435–4446. https://doi.org/10.5194/hess-16-4435-2012

Chokmani K, Ouarda TBMJ (2004) Physiographical space-based kriging for regional flood frequency estimation at ungauged sites. Water Resour Res 40(12):W12,514. https://doi.org/10.1029/2003WR002983

Cipriani T, Toilliez T, Sauquet E (2012) Estimation régionale des débits décennaux et durées caractéristiques de crue en France. La Houille Blanche 4–5:5–13. https://doi.org/10.1051/lhb/2012024

Coles S (2001) An introduction to statistical modeling of extreme values. Springer, London

Cuevas A, Febrero M, Fraiman R (2007) Robust estimation and classification for functional data via projection-based depth notions. Comput Stat 22(3):481–496. https://doi.org/10.1007/s00180-007-0053-0

Dawson CW, Abrahart RJ, Shamseldin AY, Wilby RL (2006) Flood estimation at ungauged sites using artificial neural networks. J Hydrol 319:391–409. https://doi.org/10.1016/j.jhydrol.2005.07.032

Deutsche Vereinigung für Wasserwirtschaft Abwasser und Abfall (2012) Merkblatt DWA-M 552. Tech. rep, DWA, Hennef, Germany

Diggle PJ, Ribeiro PJ Jr (2007) Model-based geostatistics. Springer series in statistics. Springer, New York

Eckhardt K (2005) How to construct recursive digital filters for baseflow separation. Hydrol Process 19:507–515. https://doi.org/10.1002/hyp.5675

Eidgenössische Forschungsanstalt für Wald Schnee und Landschaft (WSL) (1999) Schweizerisches Landesforstinventar. Ergebnisse der Zwietaufnahme 1993-1995. BUWAL, Bern

Elith J, Leathwick JR, Hastie T (2008) A working guide to boosted regression trees. J Anim Ecol 77:802–813. https://doi.org/10.1111/j.1365-2656.2008.01390.x

Farmer WH (2016) Ordinary kriging as a tool to estimate historical daily streamflow records. Hydrol Earth Syst Sci 20(7):2721–2735. https://doi.org/10.5194/hess-20-2721-2016

Freund Y, Schapire RRE (1996) Experiments with a new boosting algorithm. In: International conference on machine learning, pp 148–156, https://doi.org/10.1.1.133.1040, http://citeseerx.ist.psu.edu/viewdoc/summary?doi=10.1.1.51.6252

Friedman AJ, Hastie T, Tibshirani R (2010) Regularization paths for generalized linear models via coordiante descent. J Stat Softw 33(1):1–22

Friedman JH (2001) Greedy function approximation: a gradient boosting machine. Ann Stat 29(5):1189–1232

Friedman JH (2002) Stochastic gradient boosting. Comput Stat Data Anal 38(4):367–378

Gaál L, Kysel J, Szolgay J (2008) Region-of-influence approach to a frequency analysis of heavy precipitation in Slovakia. Hydrol Earth Syst Sci 12:825–839. https://doi.org/10.5194/hess-12-825-2008

Ganora D, Claps P, Laio F, Viglione A (2009) An approach to estimate nonparametric flow duration curves in ungauged basins. Water Resour Res 45(10):1–10. https://doi.org/10.1029/2008WR007472

Genest C, Favre AC (2007) Everything you always wanted to know about copula modeling but were afraid to ask. J Hydrol Eng 12(4):347–368. https://doi.org/10.1061/(ASCE)1084-0699(2007)12:4(347)

Gottschalk L (1993) Correlation and covariance of runoff. Stoch Hydrol Hydraul 7:85–101

Gottschalk L, Leblois E, Skoien JO (2011) Correlation and covariance of runoff revisited. J Hydrol 398:76–90. https://doi.org/10.1016/j.jhydrol.2010.12.011

Green IRA, Stephenson D (1986) Criteria for comparison of single event models. Hydrol Sci J 31(3):395–411. https://doi.org/10.1080/02626668609491056

Greene W (2002) Econometric analysis, 5th edn. Prentice Hall, New Jersey

GREHYS (1996) Presentation and review of some methods for regional flood frequency analysis. J Hydrol 186:63–84. https://doi.org/10.1016/S0022-1694(96)03042-9

Grimaldi S, Petroselli A (2015) Do we still need the Rational Formula? An alternative empirical procedure for peak discharge estimation in small and ungauged basins. Hydrol Sci J 60(1):67–77. https://doi.org/10.1080/02626667.2014.880546

Haberlandt U, Klöcking B, Krysanova V, Becker A (2001) Regionalisation of the base flow index from dynamically simulated flow

components—a case study in the Elbe River Basin. J Hydrol 248:35–53. https://doi.org/10.1016/S0022-1694(01)00391-2
Haddad K, Rahman A (2012) Regional flood frequency analysis in eastern Australia: Bayesian GLS regression-based methods within fixed region and ROI framework—quantile regression vs. parameter regression technique. J Hydrol 430–431:142–161. https://doi.org/10.1016/j.jhydrol.2012.02.012
Halkidi M, Batistakis Y, Vazirgiannis M (2001) On clustering validation techniques. J Intell Inf Syst 17(2/3):107–145. https://doi.org/10.1023/A:1012801612483
Harrell FE (2015) Regression modeling strategies. With applications to linear models, logistic and ordinal regression, and survival analysis. Springer, Cham
Hastie T, Tibshirani R, Friedman J (2008) The elements of statistical learning. Springer series in statistics. Springer, Stanford
He Y, Bardossy A, Zehe E (2011) A review of regionalisation for continuous streamflow simulation. Hydrol Earth Syst Sci 15:3539–3553. https://doi.org/10.5194/hess-15-3539-2011
Hechenbichler K, Schliep K (2004) Weighted k-nearest-neighbor techniques and ordinal classification. Mol Ecol 399:17
Hofner B, Mayr A, Robinzonov N, Schmid M (2009) Model-based Boosting in R. A Hands-on Tutorial Using the R Package mboost. Tech. rep., Department of statistics. University of Munich, Munich
Hosking JRM, Wallis JR (1993) Some statistics useful in regional frequency analysis. Water Resour Res 29(92):271–281
Hrachowitz M, Savenije HHG, Blöschl G, McDonnell JJ, Sivapalan M, Pomeroy JW, Arheimer B, Blume T, Clark MP, Ehret U, Fenicia F, Freer JE, Gelfan A, Gupta HV, Hughes DA, Hut RW, Montanari A, Pande S, Tetzlaff D, Troch PA, Uhlenbrook S, Wagener T, Winsemius HC, Woods RA, Zehe E, Cudennec C (2013) A decade of Predictions in Ungauged Basins (PUB)—a review. Hydrol Sci J 58(6):1198–1255. https://doi.org/10.1080/02626667.2013.803183
Hundecha Y, Ouarda TBMJ, Bardossy A (2008) Regional estimation of parameters of a rainfall-runoff model at ungauged watersheds using the spatial structures of the parameters within a canonical physiographic-climatic space. Water Resour Res 44(W01):427. https://doi.org/10.1029/2006WR005439
Ilorme F, Griffis VW (2013) A novel procedure for delineation of hydrologically homogeneous regions and the classification of ungauged sites for design flood estimation. J Hydrol 492:151–162. https://doi.org/10.1016/j.jhydrol.2013.03.045
James G, Witten D, Hastie T, Tibshirani R (2013) An introduction to statistical learning. With applications in R. Springer, New York. https://doi.org/10.1007/978-1-4614-7138-7
Jensen H, Lang H, Rinderknecht J (1997) Extreme point rainfall of varying duration and return period 1901–1970. In: Hydrological Atlas of Switzerland, FOEN, Bern, chap 2.4
Ji Z, Li N, Xie W, Wu J, Zhou Y (2013) Comprehensive assessment of flood risk using the classification and regression tree method. Stoch Env Res Risk Assess 27(8):1815–1828. https://doi.org/10.1007/s00477-013-0716-z
Joe H (1997) Multivariate models and dependence concepts. Chapman and Hall/CRC, London
Kiers HAL, Smilde AK (2007) A comparison of various methods for multivariate regression with highly collinear variables. Stat Methods Appl 16:193–228. https://doi.org/10.1007/s10260-006-0025-5
Kjeldsen TR, Jones DA (2010) Predicting the index flood in ungauged UK catchments: on the link between data-transfer and spatial model error structure. J Hydrol 387(1–2):1–9. https://doi.org/10.1016/j.jhydrol.2010.03.024
Kokkonen TS, Jakeman AJ, Young PC, Koivusalo HJ (2003) Predicting daily flows in ungauged catchments: model regionalization from catchment descriptors at the Coweeta Hydrologic Laboratory, North Carolina. Hydrol Process 17(11):2219–2238. https://doi.org/10.1002/hyp.1329
Laaha G, Blöschl G (2006) A comparison of low flow regionalisation methods-catchment grouping. J Hydrol 323(1–4):193–214. https://doi.org/10.1016/j.jhydrol.2005.09.001
Laaha G, Skoien JO, Blöschl G (2014) Spatial prediction on river networks: comparison of top-kriging with regional regression. Hydrol Process 28:315–324. https://doi.org/10.1002/hyp.9578
Lang M, Ouarda T, Bobée B (1999) Towards operational guidelines for over-threshold modeling. J Hydrol 225:103–117
Le Cessie S, van Houwelingen JC (1992) Ridge estimators in logistic regression. J Appl Stat 41(1):191–201. https://doi.org/10.2307/2347628
Liaw A, Wiener M (2002) Classification and regression by randomForest. R News 2(3):18–22
Longobardi A, Villani P (2008) Baseflow index regionalization analysis in a Mediterranean area and data scarcity context: role of the catchment permeability index. J Hydrol 355:63–75. https://doi.org/10.1016/j.jhydrol.2008.03.011
Lu GY, Wong DW (2008) An adaptive inverse-distance weighting spatial interpolation technique. Comput Geosci 34(9):1044–1055. https://doi.org/10.1016/j.cageo.2007.07.010
Matheron G (1971) The theory of regionalized variables and its applications, vol 5. École nationale supérieure des Mines, Paris
McIntyre N, Lee H, Wheater H, Young A, Wagener T (2005) Ensemble predictions of runoff in ungauged catchments. Water Resour Res 41(12):1–14. https://doi.org/10.1029/2005WR004289
Mediero L, Jiménez-Alvarez A, Garrote L (2010) Design flood hydrographs from the relationship between flood peak and volume. Hydrol Earth Syst Sci 14:2495–2505. https://doi.org/10.5194/hess-14-2495-2010
Merz R (2006) Regionalisierung von statistischen Hochwasserkenngrössen. In: Godina R, Blöschl G (eds) Methoden der hydrologischen Regionalisierung, vol 197. Wiener Mitteilungen, Wien, pp 109–130
Merz R, Blöschl G (2003) A process typology of regional floods. Water Resour Res 39(12):1340. https://doi.org/10.1029/2002WR001952
Merz R, Blöschl G (2004) Regionalisation of catchment model parameters. J Hydrol 287(1):95–123. https://doi.org/10.1016/j.jhydrol.2003.09.028
MeteoSwiss (2013) Documentation of MeteoSwiss grid-data products: Daily precipitation (final analysis): RhiresD. Tech. rep., MeteoSwiss, http://www.meteoschweiz.admin.ch/web/de/services/datenportal/gitterdaten/precip/rhiresd.Par.0007.DownloadFile.tmp/proddocrhiresd.pdf
Mevik BH, Wehrens R (2007) The pls package: principal component and partial least squares regression in R. J Stat Softw 18(2):1–23. https://doi.org/10.18637/jss.v018.i02
Meylan P, Favre AC, Musy A (2012) Predictive hydrology. A frequency analysis approach. Science Publishers, St. Helier, Jersey, British Channel Islands
Myers RH, Montgomery DC, Vining GG, Robinson TJ (2010) Generalized Linear Models, vol 4. Wiley, Hoboken
Nathan RJ, McMahon TA (1990) Identification of homogeneous regions for the purposes of regionalisation. J Hydrol 121:217–238
Nied M, Pardowitz T, Nissen K, Ulbrich U, Hundecha Y, Merz B (2014) On the relationship between hydro-meteorological patterns and flood types. J Hydrol 519:3249–3262. https://doi.org/10.1016/j.jhydrol.2014.09.089
Osborne JW (2010) Improving your data transformations: applying the Box-Cox transformation. Pract Assess Res Eval 15(12):1–9
Ouarda T, Cunderlik JM, St-Hilaire A, Barbet M, Bruneau P, Bobée B (2006) Data-based comparison of seasonality-based regional

flood frequency methods. J Hydrol 330(1):329–339. https://doi.org/10.1016/j.jhydrol.2006.03.023
Ouarda TBMJ, Haché M, Bruneau P, Bobée B (2000) Regional flood peak and volume estimation in northern Canadian basin. J Cold Reg Eng 14:176–191. https://doi.org/10.1061/(ASCE)0887-381X(2000)14:4(176)
Ouarda TBMJ, Girard C, Cavadias GS, Bobée B (2001) Regional flood frequency estimation with canonical correlation analysis. J Hydrol 254:157–173
Oudin L, Andréassian V, Perrin C, Michel C, Moine NL (2008) Spatial proximity, physical similarity, regression and ungaged catchments: A comparison of regionalization approaches based on 913 French catchments. Water Resour Res 44:W03, 413. https://doi.org/10.1029/2007WR006240
Oudin L, Kay A, Andréassian V, Perrin C (2010) Are seemingly physically similar catchments truly hydrologically similar? Water Resour Res 46(W11):558. https://doi.org/10.1029/2009WR008887
Parajka J, Merz R, Blöschl G (2005) A comparison of regionalisation methods for catchment model parameters. Hydrol Earth Syst Sci 9:157–171. https://doi.org/10.5194/hess-9-157-2005
Parajka J, Andréassian V, Archfield SA, Bardossy A, Blöschl G, Chiew F, Duan Q, Gelfan A, Hlavconva K, Merz R, McIntyre N, Oudin L, Perrin C, Rogger M, Salinas JL, Savenije HG, Skoien JO, Wagener T, Zehe E, Zhang Y (2013) Prediction of runoff hydrographs in ungauged basins. In: Blöschl G, Sivapalan M, Wagener T, Viglione A, Savenije H (eds) Predictions in ungauged basins. A synthesis across processes, places and scales, Cambridge University Press, Cambridge, pp 227–269
Pebesma E (2004) Multivariable geostatistics in S: the gstat package. Comput Geosci 30:683–691. https://doi.org/10.1016/j.cageo.2004.03.012
Peters A, Hothorn T, Ripley BD, Therneau T, Atkinson B (2015) Package ' ipred ' : improved predictors. http://cran.r-project.org/package=ipred
Petroselli A, Grimaldi S (2015) Design hydrograph estimation in small and fully ungauged basins: a preliminary assessment of the EBA4SUB framework. J Flood Risk Manag. https://doi.org/10.1111/jfr3.12193
Pilgrim DH (1986) Bridging the gap between flood research and design practice. Water Resour Res 22(9):165–176
Prinzio MD, Castellarin A, Toth E (2011) Data-driven catchment classification: application to the pub problem. Hydrol Earth Syst Sci 15:1921–1935. https://doi.org/10.5194/hess-15-1921-2011
R Core Team (2015) R: a language and environment for statistical computing. http://www.r-project.org/
Rahman A, Charron C, Ouarda TBMJ, Chebana F (2017) Development of regional flood frequency analysis techniques using generalized additive models for Australia. Stoch Environ Res Risk Assess pp 1–17, https://doi.org/10.1007/s00477-017-1384-1
Rai RK, Sarkar S, Singh VP (2009) Evaluation of the adequacy of statistical distribution functions for deriving unit hydrograph. Water Resour Manage 23:899–929. https://doi.org/10.1007/s11269-008-9306-0
Rasmussen PF, Bobée B, Bernier J (1993) Une méthodologie générale de comparaison de modèles d'estimation régionale de crue. Revue des sciences de l'eau 7:23–41. https://doi.org/10.7202/705187ar
Razavi T, Coulibaly P (2013) Streamflow prediction in ungauged basins: review of regionalization methods. J Hydrol Eng 18(8):958–975. https://doi.org/10.1061/(ASCE)HE.1943-5584.0000690
Requena AI, Mediero L, Garrote L (2013) A bivariate return period based on copulas for hydrologic dam design: accounting for reservoir routing in risk estimation. Hydrol Earth Syst Sci 17:3023–3038. https://doi.org/10.5194/hess-17-3023-2013
Ridgeway G (2007) Generalized boosted models: a guide to the gbm package. Compute 1(4):1–12. https://doi.org/10.1111/j.1467-9752.1996.tb00390.x
Rosbjerg D, Blöschl G, Burn DH, Castellarin A, Croke B, Baldassarre GD, Iacobellis V, Kjeldsen TR, Kuczera G, Merz R, Montanari A, Morris D, Ouarda T, Ren L, Rogger M, Salinas JL, Toth E, Viglione A (2013) Prediction of floods in ungauged basins. In: Blöschl G, Sivapalan M, Wagener T, Viglione A, Savenije H (eds) Runoff prediction in ungauged basins. A synthesis across processes, places and scales, Cambridge University Press, Cambridge, chap 9, pp 189–226
Salinas JL, Laaha G, Rogger M, Parajka J, Viglione A, Sivapalan M, Blöschl G (2013) Comparative assessment of predictions in ungauged basins—Part 2: flood and low flow studies. Hydrol Earth Syst Sci 17:2637–2652. https://doi.org/10.5194/hess-17-2637-2013
Samuel J, Coulibaly P, Metcalfe RA (2011) Estimation of continuous streamflow in ontario ungauged basins: comparison of regionalization methods. J Hydrol Eng 16(5):447–459. https://doi.org/10.1061/(ASCE)HE.1943-5584.0000338
Sauquet E (2006) Mapping mean annual river discharges: geostatistical developments for incorporating river network dependencies. J Hydrol 331:300–314. https://doi.org/10.1016/j.jhydrol.2006.05.018
Sauquet E, Catalogne C (2011) Comparison of catchment grouping methods for flow duration curve estimation at ungauged sites in France. Hydrol Earth Syst Sci 15:2421–2435. https://doi.org/10.5194/hess-15-2421-2011
Sefton CEM, Howarth SM (1998) Relationships between dynamic response characteristics and physical descriptors of catchments in England and wales. J Hydrol 211(1–4):1–16. https://doi.org/10.1016/S0022-1694(98)00163-2
Serinaldi F, Grimaldi S (2011) Synthetic design hydrographs based on distribution functions with finite support. J Hydrol Eng 16:434–446. https://doi.org/10.1061/(ASCE)HE.1943-5584.0000339
Shapiro SS, Wilk MB (1965) An analysis of variance test for normality (complete samples). Biometrika 52(34):591–611
Shiau J, Wang HY, Tsai CT (2006) Bivariate Frequency Analysis of floods using copulas. J Am Water Resour Assoc pp 1549–1564, https://doi.org/10.1111/j.1752-1688.2006.tb06020.x
Shu C, Burn DH (2004) Artificial neural network ensembles and their application in pooled flood frequency analysis. Water Resour Res 40(9):1–10. https://doi.org/10.1029/2003WR002816
Shu C, Ouarda T (2008) Regional flood frequency analysis at ungauged sites using the adaptive neuro-fuzzy inference system. J Hydrol 349:31–43. https://doi.org/10.1016/j.jhydrol.2007.10.050
Sikorska AE, Viviroli D, Seibert J (2015) Flood type classification in mountainous catchments using crisp and fuzzy decision trees. Water Resour Res 51(10):7959–7976. https://doi.org/10.1002/2015WR017326
Singh PK, Mishra SK, Jain MK (2014) A review of the synthetic unit hydrograph: from the empirical UH to advanced geomorphological methods. Hydrol Sci J. https://doi.org/10.1080/02626667.2013.870664
Sivapalan M (2003) Prediction in ungauged basins: a grand challenge for theoretical hydrology. Hydrol Process 17:3163–3170. https://doi.org/10.1002/hyp.5155
Skoien JO, Merz R, Blöschl G (2006) Top-kriging—geostatistics on stream networks. Hydrol Earth Syst Sci 10:277–287. https://doi.org/10.5194/hess-10-277-2006
Skoien JO, Blöschl G, Laaha G, Pebesma E, Parajka J, Viglione A (2014) An R package for interpolation of data with a variable spatial support, with an example from river networks. Comput Geosci 67:180–190

Smithers JC (2012) Methods for design flood estimation in South Africa. Water SA 38(4):633–646. https://doi.org/10.4314/wsa.v38i4.19

Steinschneider S, Yang YCE, Brown C (2014) Combining regression and spatial proximity for catchment model regionalization: a comparative study. Hydrol Sci J 6667:1–18. https://doi.org/10.1080/02626667.2014.899701

Strobl C, Malley J, Tutz G (2009) An introduction to recursive partitioning: rationale, application and characteristics of classification and regression trees, bagging and random forests. Psychol Methods 14(4):323–348. https://doi.org/10.1037/a0016973

Takezawa K (2012) Introduction to nonparametric regression. Wiley, Hoboken, https://doi.org/10.1021/cr2001349

Tibshirani R (1997) The lasso method for variable selection in the Cox model. Stat Med 16(4):385–395. https://doi.org/10.1002/(SICI)1097-0258(19970228)16:4%3c385::AID-SIM380%3e3.0.CO;2-3

Tung YK, Yeh KC, Yang JC (1997) Regionalization of unit hydrograph parameters: 1. Comparison of regression analysis techniques. Stoch Hydrol Hydraul 11:145–171

Viglione A, Merz R, Blöschl G (2009) On the role of the runoff coefficient in the mapping of rainfall to flood return periods. Hydrol Earth Syst Sci 6(1):627–665. https://doi.org/10.5194/hessd-6-627-2009

Viviroli D, Mittelbach H, Gurtz J, Weingartner R (2009a) Continuous simulation for flood estimation in ungauged mesoscale catchments of Switzerland—Part II: parameter regionalisation and flood estimation results. J Hydrol 377:208–225. https://doi.org/10.1016/j.jhydrol.2009.08.022

Viviroli D, Zappa M, Gurtz J, Weingartner R (2009b) An introduction to the hydrological modelling system PREVAH and its pre-and post-processing-tools. Environ Model Softw 24:1209–1222. https://doi.org/10.1016/j.envsoft.2009.04.001

Webster R, Oliver MA (2007) Geostatistics for environmental scientists. Statistics in practice. Wiley, Chichester

Weisberg S (2005) Applied Linear Regression, 3rd edn. Wiley, Hoboken

Yamamoto JK (2007) On unbiased backtransform of lognormal kriging estimates. Comput Geosci 11:219–234. https://doi.org/10.1007/s10596-007-9046-x

Yue S, Rasmussen P (2002) Bivariate frequency analysis: discussion of some useful concepts in hydrological application. Hydrol Process 16:2881–2898. https://doi.org/10.1002/hyp.1185

Yue S, Ouarda T, Bobée B, Legendre P, Bruneau P (2002) Approach for describing statistical properties of flood hydrograph. J Hydrol Eng 7(2):147–153. https://doi.org/10.1061/(ASCE)1084-0699(2002)7:2(147)

Zhang Y, Chiew FHS (2009) Relative merits of different methods for runoff predictions in ungauged catchments. Water Resour Res 45(W07):412. https://doi.org/10.1029/2008WR007504